Flux analysis, the correspondence principle, and the structure of quantum phase space

Rex T. Skodje, Henry W. Rohrs, and James VanBuskirk
Department of Chemistry and Biochemistry, University of Colorado, Boulder, Colorado 80309-0215
(Received 8 March 1989)

The hydrodynamic analogy for quantum mechanics is developed in a quantum phase-space representation. The key technical step in this development is the formulation of a phase-space flux (or current) density expression. Lagrangian fluid trajectories in phase space are explicitly found as solutions to a set of first-order ordinary differential equations which are formulated without making semiclassical approximation to the quantum dynamics. These fluid trajectories may be used to construct sharp structures in quantum phase space in the same way that one uses classical trajectories in classical mechanics. While these sharp structures do not themselves represent states, their properties "control" the dynamics of states in a manner familiar from the theory of first-order flows. The formalism reduces to Liouville dynamics in the classical limit, $\hbar \to 0$. In addition to several analytic applications to the pure- and mixed-state dynamics, the approach is numerically implemented for tunneling dynamics in a double-well problem. A new picture for quantum tunneling emerges where the tunneling transport occurs when density spirals outward from one well along real-valued fluid trajectories and then into the other well. The tunneling is found to occur through localized portals, or "flux gates" in the phase space. We advocate the phase-space hydrodynamic model as a general tool to understand classical quantum correspondence.

I. INTRODUCTION

The study of classical-quantum correspondence has intensified in recent time[1,2] due in part to the profound advances that have occurred in our understanding of classical nonlinear dynamics. In particular, significant interest has developed for the study of quantum manifestations of classical phase-space structure.[1-32] The results of numerous studies have made it quite clear that quantum dynamics is often strongly influenced by the presence of structures in the classical phase space such as Kolmogorov-Arnold-Moser (KAM) surfaces, cantori, separatrices, islands of nonlinear resonance, and homoclinic tangle. The correspondence can be especially striking when the quantum dynamics is cast into a "quantum phase-space representation"[33-53] where one may observe the quantum density apparently being molded by an underlying classical-like phase-space structure (Refs. 6, 8–10, 13, 18, 20, 21, 24–26, and 29). The uncertainty principle does not allow a unique definition of quantum phase space and thus an infinite number of these formulations may be constructed. Examples of such representations include the Wigner equivalent representation, the coherent-state (or Husimi) representation, the Glauber-Sudarshan diagonal-P representation, and various off-diagonal generalized-P representations. Despite this ambiguity, quantum phase-space theories provide an attractive approach to the study of quantum chaos and the correspondence principle since phase space provides the proper setting for studying nonlinear dynamics.

To illustrate the typical behavior one observes in quantum phase-space representations, we consider the motion of a wave packet in a one-degree-of-freedom quartic double-well potential. The potential curve and the associated classical phase-space structure are depicted in Fig. 1. The initial wave packet is chosen as a Gaussian. Its mean energy is somewhat less than the barrier height and it is centered at an outer turning point of a classical orbit of that energy. The wave packet is then numerically propagated to high accuracy and, at regular time intervals, the packet is transformed into the coherent-state quantum phase-space representation yielding a time-dependent quasi-probability-density. This transformation is easily accomplished by taking the overlap of a coherent state centered at the point (p,q) in "phase space" (see Sec. II for the details) with the evolving wave packet and squaring, i.e.,

$$\rho(p,q,t)=|\langle p,q|\Psi\rangle|^2 . \tag{1.1}$$

The contours of ρ at a series of times are shown in Fig. 2. Even though Planck's constant is not particularly small in the scale of this system (there are eight states below the barrier), the influence of the classical phase-space structure on the quantum evolution is clearly apparent from the plot, especially at early times. For example, one can see density following the separatrix in the first six panels.

Even though the classical-quantum correspondence is often evident, systematic procedures are lacking to directly construct the quantum phase-space structures, even given the exact wave functions. Thus one might see a separatrix or a KAM curve manifested in ρ, as in Fig. 2, but not be able to explicitly construct it. One reason for this is a common belief that sharp phase-space structures cannot exist or are not meaningful in quantum mechanics due to so called $\hbar$ smoothing.[6] Hence one instead often encounters references to items like "fuzzy KAM curves," etc., which are suppose to be the analogs

of classical structures but occupy phase-space volumes of order $\hbar^N$. Our thesis in this paper is that meaningful sharp structure in quantum phase-space representations does exist, can be explicitly constructed from a knowledge of the wave function, and can be profitably used to interpret quantum dynamics. The existence of such structure is not in conflict with the results of Berry *et al.*[6] on $\hbar$ smoothing since the sharp structures we construct do not represent states. Instead, they are zero measure structures in the quantum phase space, which do not lie in the Hilbert space of states, but nevertheless control the behavior of volumes of phase space and hence control the dynamics of states. (The use of such zero measure objects in quantum mechanics is not unprecedented. Recall, e.g., the work of Gutzwiller[54] on the quantum significance of periodic orbits.)

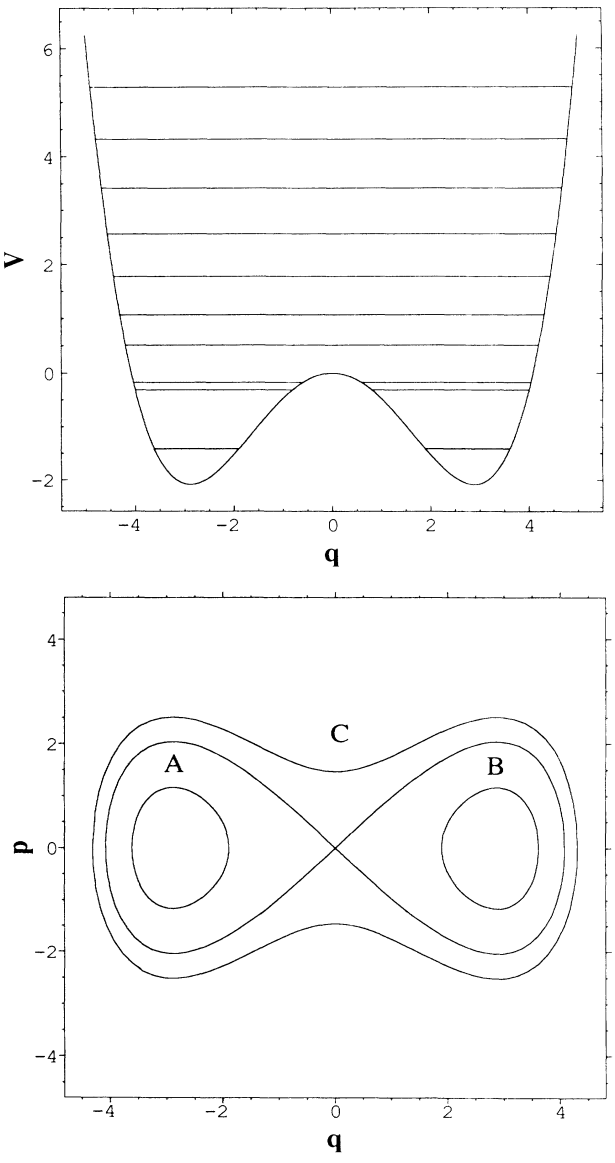

FIG. 1. The upper panel shows the double-well potential. The positions of the eigenstates used in the calculations of Sec. IV are depicted. The lower panel shows the classical phase-space structure for the system. A figure-eight separatrix divides the phase space into three disjoint regions labeled *A*, *B*, and *C*.

We base our approach on a reformulation of the hydrodynamic interpretation of quantum mechanics.[55–67] The hydrodynamic model, originally proposed by Madelung,[55] provides a classical picture for quantum dynamics, namely, that of the flow of an indestructible probability fluid. In this picture, one may consistently interpret the time evolution of the density $\rho(\mathbf{x},t)=|\Psi(\mathbf{x},t)|^2$ as a fluid being continuously driven along fluid trajectories by a current density $\mathbf{j}(\mathbf{x},t)$. In the limit $\hbar\rightarrow 0$, the fluid trajectories become the configuration space orbits of classical trajectories. The key relation that validates this interpretation is the continuity equation

$$\frac{\partial\rho(\mathbf{x},t)}{\partial t}=-\nabla\cdot\mathbf{j}(\mathbf{x},t)\ , \tag{1.2}$$

which is easily derived from the Schrödinger equation. We review the details of the quantum hydrodynamic analogy in Sec. II A.

For classical Hamiltonian mechanics, it is well known that the hydrodynamic analogy should be invoked in phase space. Specifically, the evolution of an ensemble with probability density $f(\mathbf{p},\mathbf{q},t)$ can be interpreted as the flow of an incompressible ideal fluid. The dynamics is governed by the Liouville equation,

$$\frac{\partial f}{\partial t}=\sum_{i=1}^{N}\left[\frac{\partial H}{\partial q}\frac{\partial f}{\partial p_i}-\frac{\partial f}{\partial q_i}\frac{\partial H}{\partial p_i}\right]\ , \tag{1.3}$$

which is equivalent to a continuity equation in phase space,

$$\frac{\partial f}{\partial t}=-\nabla\cdot\mathbf{J}\ , \tag{1.4}$$

with the identifications $\nabla=(\nabla_p,\nabla_q)$ and $\mathbf{J}=(f\dot{\mathbf{p}},f\dot{\mathbf{q}})=(-f\nabla_q H,f\nabla_p H)$. The fluid orbits lie along classical trajectories in phase space. The density f is constant along an evolving trajectory since phase-space volumes are invariant.

We propose to calculate the fluid trajectories for the quantum fluid and use these trajectories to map out the structure of the quantum phase space. The philosophy of the approach is quite simple and we illustrate it first for the classical case. Imagine that $f(\mathbf{p},\mathbf{q},t)$ and the flux density $\mathbf{J}(\mathbf{p},\mathbf{q},t)$ are known to us, say provided numerically, but we are not given the explicit Hamiltonian function or its derivatives. We can still find the fluid trajectories by first defining the velocity field $\mathbf{v}(\mathbf{p},\mathbf{q},t)\equiv(\mathbf{v}_p(\mathbf{p},\mathbf{q},t),\mathbf{v}_q(\mathbf{p},\mathbf{q},t))$ as

$$\mathbf{v}(\mathbf{p},\mathbf{q},t)=\mathbf{J}(\mathbf{p},\mathbf{q},t)/f(\mathbf{p},\mathbf{q},t)\ , \tag{1.5}$$

when $f\neq 0$, and then solving the defining equations,

$$\begin{aligned}\frac{d\mathbf{p}}{dt}&=\mathbf{v}_p(\mathbf{p},\mathbf{q},t)\ ,\\ \frac{d\mathbf{q}}{dt}&=\mathbf{v}_q(\mathbf{p},\mathbf{q},t)\ .\end{aligned} \tag{1.6}$$

For the classical phase-space fluid, these are just Hamilton's equations. In the special case where the classical Hamiltonian takes the form $H=\mathbf{p}^2/2m+V(\mathbf{q})$, the velocity field $\mathbf{v}_q$ is the configuration space velocity, while the field $\mathbf{v}_p$ is equal to the force field. In quantum mechanics, on the other hand, we will know the probability and flux densities from the wave function, which is given, but $\mathbf{v}$ will not reduce to a simple analytic function.

The quantum hydrodynamic model of Madelung is expressed in configuration space. The quantum trajectories associated with this theory may be readily found but are not useful in determining phase-space structure. To make use of the simple scheme presented above, it is necessary to cast the hydrodynamic model into a quantum phase-space representation. This is not trivial and most of the formal work in this paper is devoted to accomplishing this. We explicitly develop this theory for the coherent-state representation, although we have also implemented the approach for the Wigner representation (to be presented elsewhere). Thus the fluid density is the non-negative quasi-probability-density $\rho(\mathbf{p},\mathbf{q},t)$, Eq. (1.1). The main effort is devoted to formulating the flux density. We develop a nonlocal flux operator for phase space and the coherent-state representation of this operator is the desired flux density.

We note that dynamics in quantum phase-space repre-

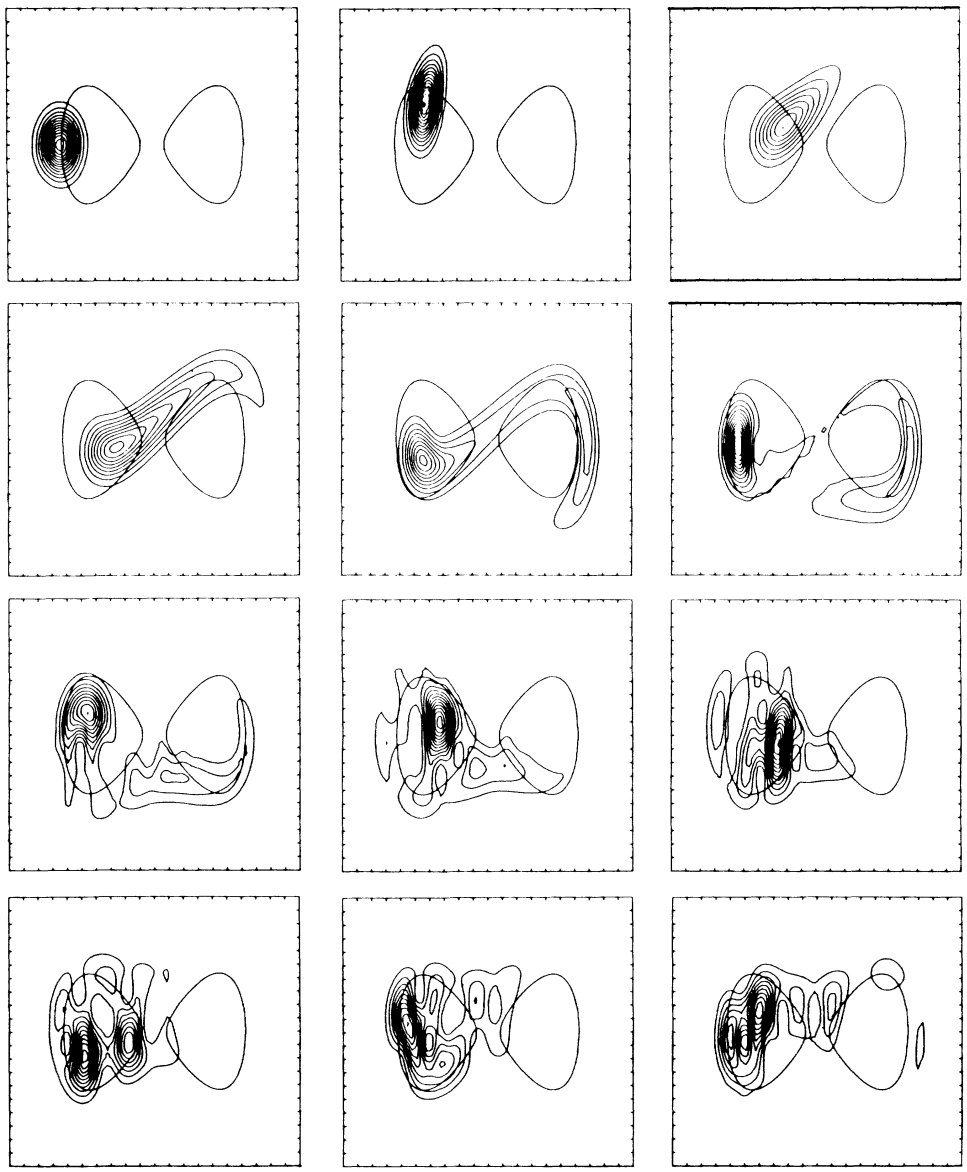

FIG. 2. Exact quantum evolution of the coherent-state density ρ for an initial Gaussian wave packet in a quartic double-well potential [the Hamiltonian is Eq. (4.1) with $\gamma=\frac{1}{100}$]. The different panels show the density in (p,q) space at the set of equally spaced times $t=n\tau_{\text{vib}}/10$, $n=0,1,\ldots,$ where τ_{vib} is the harmonic period for the bottom of the single well.

sentations has been studied often before, starting with Wigner in 1932.[6,9,21,33,36,42–45,47–50] Much of this work has centered on the development and study of the "quantum Liouville equation," which is an infinite-order partial differential equation for the time-dependent quasi-probability-density. We adopt a different approach in this work based on a flux analysis in quantum phase space. The central relation we derive is a first-order phase-space continuity equation connecting ρ and $\mathbf{J}$, which justifies the hydrodynamic analogy. With appropriate substitutions and Taylor expansions and using implicit assumptions about analyticity, $\mathbf{J}$ can be eliminated in favor of ρ and the continuity equation can be shown to be equivalent to the quantum Liouville equation. However, our procedure of retaining both ρ and $\mathbf{J}$ is more useful in the present case since the fluid trajectories are obtained in a simple way from the velocity field, while they cannot be easily computed from the quantum Liouville equation. We also emphasize the difference in motivation between our work and that of most of the previous work. Most previous work has stressed using the quantum Liouville equation to actually solve for ρ or to estimate quantum corrections to the Liouville equation. Here, the wave function is given and thus ρ and $\mathbf{J}$ are already known, and we carry out the analysis in order to reveal the structure of quantum phase space.

Now that we have briefly outlined our approach, we direct attention back to the dynamics in Fig. 2. We imagine the fluid density ρ being driven along fluid trajectories by an underlying current density. Intuitively, the quantum trajectories will surely bear some important similarities to the classical trajectories shown in Fig. 1. Indeed, one may even semiquantitatively account for aspects of the short-time evolution of ρ using the classical Liouville equation. Of course there must also be important differences between classical and quantum description in order to account for nonclassical effects such as tunneling and interference. The proposed approach allows us to directly obtain the quantum phase-space structure without reference to the classical problem. The quantum dynamics has been written in the form of a set of coupled first-order ordinary differential equations (ODE's), the trajectory equations (1.6), and thus much of well-developed methodology for studying first-order flows may be employed.[68,69] For example, fixed-point analyses may be carried out, and return maps constructed. Using the fluid orbits in the same general way one uses classical trajectories,[68,69] one can construct sharp phase-space structures such as fixed points, separatrices, and cantori. These structures do not themselves represent states, which must occupy certain minimal volumes in phase space, but instead govern the dynamics of states in the same way that such structures control the dynamics in any first-order flow.

The remainder of this article is organized as follows. Section II presents the formal treatment of the hydrodynamic analogy. It begins with a brief review of the standard hydrodynamic analogy for pure states in configuration space. Then the hydrodynamic analogy is successively extended to mixed states, to the momentum-space representation, and finally to dynamics in quantum phase-space representations. In Sec, III, the general characteristics of the quantum phase-space hydrodynamic model are discussed. The behavior of the formalism near the correspondence limit is then derived and the concept of a "flux gauge" is discussed. The method is then analytically applied to the free particle and the harmonic oscillator. In Sec. IV the method is numerically applied to the dynamics of wave packets in a quartic double-well potential. The relevant nonlinear phase-space structure is numerically constructed using the Lagrangian fluid trajectories. Making practical use of the numerical phase-space structure, we calculate high accuracy tunneling rates by computing the one way flux through localized "flux gates." Section V contains our conclusions. The Appendix presents an alternative formalism for the extension of hydrodynamic analogy to mixed states and to quantum phase-space patterned on Madelung's original approach.

II. FORMAL DEVELOPMENT OF THE HYDRODYNAMIC MODEL IN QUANTUM PHASE SPACE

A. Review of configuration-space hydrodynamic model

In order to motivate our treatment, we begin with a brief review of the well-established hydrodynamic analogy for configuration space.[55–67] Consider first the pure state quantum dynamics generated by the N-degree-of-freedom nonrelativistic Schrödinger equation,

$$\hat{H}\Psi(\mathbf{x},t)=i\hbar\frac{\partial\Psi(\mathbf{x},t)}{\partial t}\ , \tag{2.1}$$

where $\mathbf{x}=(x_1,\ldots,x_N)$. For simplicitly, it shall be assumed that $\hat{H}$ may be put into the form

$$\hat{H}=\frac{1}{2m}\sum_{n=1}^{N}\hat{\mathbf{P}}_n^2+V(\mathbf{x}) \tag{2.2}$$

in a mass-scaled Cartesian coordinate system. The analysis is facilitated by writing the wave function in the form

$$\Psi(\mathbf{x},t)=Ae^{iS/\hbar}\ , \tag{2.3}$$

where A and S are well-behaved real-valued functions of $\mathbf{x}$ and t. The imaginary and real parts of the Schrödinger equation then give the independent relations

$$\frac{\partial\rho_x(\mathbf{x},t)}{\partial t}=-\nabla_x\cdot\mathbf{j}_x(\mathbf{x},t)\ , \tag{2.4}$$

$$\frac{\partial S(\mathbf{x},t)}{\partial t}=\frac{1}{2m}[\nabla_x S(\mathbf{x},t)]^2+V(x)-\frac{\hbar^2\nabla_x^2 A(\mathbf{x},t)}{2mA(\mathbf{x},t)}\ , \tag{2.5}$$

where the probability density $\rho_x(\mathbf{x},t)$ and the current density $\mathbf{j}_x(\mathbf{x},t)$ can be related to the wave function in the usual way,

$$\rho_x(\mathbf{x},t)=|\Psi(\mathbf{x},t)|^2=A(\mathbf{x},t)^2\ , \tag{2.6}$$

$$\mathbf{j}_x(\mathbf{x},t)=\frac{\hbar}{2mi}[\Psi^*(\mathbf{x},t)\nabla_x\Psi(\mathbf{x},t)-\Psi(\mathbf{x},t)\nabla_x\Psi^*(\mathbf{x},t)]$$
$$=\rho_x(\mathbf{x},t)\frac{\nabla_x S(\mathbf{x},t)}{m}\ . \tag{2.7}$$

(To avoid future confusion, the subscript x has been add-

ed to quantities in this configuration-space analysis.) Equations (2.4) is the continuity equation, which is the minimal requirement for the interpretation as an indestructible fluid. The hydrodynamic analogy can be emphasized even more by rewriting Eq. (2.5) in differential form,

$$\frac{d\mathbf{v}_x(\mathbf{x},t)}{dt}\equiv\frac{\partial\mathbf{v}_x(\mathbf{x},t)}{\partial t}+[\mathbf{v}_x(\mathbf{x},t)\cdot\nabla_x]\mathbf{v}_x(\mathbf{x},t)$$
$$=\frac{-1}{m}\nabla_x\left[V(\mathbf{x})-\frac{\hbar^2\nabla_x^2[\rho_x(\mathbf{x},t)]^{1/2}}{2m[\rho_x(\mathbf{x},t)]^{1/2}}\right], \quad (2.5')$$

where $\mathbf{v}_x(\mathbf{x},t)$ is the velocity field

$$\mathbf{v}_x(\mathbf{x},t)\equiv\mathbf{j}_x(\mathbf{x},t)/\rho_x(\mathbf{x},t) . \quad (2.8)$$

Relation (2.5′) is then Euler's equation for the flow of a compressible ideal (inviscid) fluid.[70] Equation (2.5′) states that each element of the fluid moves under the influence of the external potential $V(\mathbf{x})$ as well as an internal quantum pressure potential $-(\hbar^2/2m)\nabla_x^2\sqrt{\rho_x}/\sqrt{\rho_x}$. The quantum dynamics may, in principle, be obtained in the hydrodynamic picture by solving Eqs. (2.4) and (2.5′) for the fluid flow variables ρ_x and $\mathbf{j}_x$, which can be related back to the wave function using (2.6) and (2.7). Of course, our eventual strategy will be to solve the Schrödinger equation in some other more efficient way and use a hydrodynamic model to interpret the quantum dynamics.

Not every fluid configuration $(\rho_x,\mathbf{j}_x)_0$ that one could write down at an instant t_0 corresponds to a quantum state. In particular, the requirement that the wave function be single valued implies that the line integral of the velocity field around any closed contour be zero or some integer multiple of $2\pi\hbar/m$, i.e.,

$$\oint_C \mathbf{v}_x(\mathbf{x},t_0)\cdot d\mathbf{s}=\oint_C\frac{\nabla_x S(\mathbf{x},t_0)}{m}\cdot d\mathbf{s}=\frac{2\pi n\hbar}{m},$$
$$n=0,\pm1,\pm2,\ldots . \quad (2.9)$$

When $n=0$, the velocity field is irrotational. When $n\neq0$, there exists a quantized whirlpool in the fluid flow. The existence of quantized whirlpools was first discussed by Dirac in his classic paper on magnetic monopoles[57] and has been subsequently studied in more detail.[60,62,63,67] It has been found that quantized whirlpools are intimately related to nodes in the wave function. This is easily appreciated through a brief consideration of (2.9). For an infinitesimal contour loop C, away from any node, n must be zero in (2.9). If C is gradually expanded, then n must remain zero by continuity unless $\mathbf{v}_x$ diverges. In general, $\mathbf{v}_x=\mathbf{j}_x/\rho$ diverges only at nodes since there $\rho=0$ and $\mathbf{j}_x$ approaches zero more slowly than ρ (since $\mathbf{j}_x\sim\mathrm{Im}\Psi^*\nabla\Psi$, $\Psi^*=0$ but $\nabla\Psi\neq0$), and thus the line integral can jump by quantized amounts at nodes. Thus, one generally has quantized whirlpools encircling nodal lines.

B. Operator formalism

We most easily generalize the hydrodynamic analogy to mixed states and to more general representations by recasting the formalism into an operator language. Thus we consider the dynamics of a density operator $\hat{\rho}$ which satisfies the Von Neumann equation

$$i\hbar\frac{\partial\hat{\rho}}{\partial t}=[\hat{H},\hat{\rho}] . \quad (2.10)$$

We shall consider here only the diagonal dynamics of Eq. (2.10) using the expectation value

$$\left\langle\mathbf{x}\left|\frac{\partial\hat{\rho}}{\partial t}\right|\mathbf{x}\right\rangle=\frac{1}{i\hbar}\langle\mathbf{x}|[\hat{H},\hat{\rho}]|\mathbf{x}\rangle . \quad (2.11)$$

The hydrodynamic analogy for the off-diagonal dynamics may also be developed (see the Appendix) by working in a $2N$-dimensional configuration space. Inserting the Hamiltonian (2.2) into Eq. (2.11), we obtain the continuity equation

$$\frac{\partial\rho_x(\mathbf{x},t)}{\partial t}=-\nabla_x\cdot\mathbf{j}_x(\mathbf{x},t) . \quad (2.12)$$

The probability and current densities are given by

$$\rho_x(\mathbf{x},t)\equiv\rho(\mathbf{x},\mathbf{x},t) , \quad (2.13)$$

with

$$\rho(\mathbf{x},\mathbf{y},t)\equiv\langle\mathbf{x}|\hat{\rho}|\mathbf{y}\rangle ,$$

and

$$\mathbf{j}_x(\mathbf{x},t)\equiv\frac{\hbar}{2mi}[\nabla_x\rho(\mathbf{x},\mathbf{y},t)-\nabla_y\rho(\mathbf{x},\mathbf{y},t)]_{y=x} . \quad (2.14)$$

In analogy to the expression (2.13), the current density (2.14) may also be obtained by the position expectation of a configuration space *flux density* operator $\hat{\mathbf{j}}_x$,

$$\mathbf{j}_x(\mathbf{x},t)=\langle\mathbf{x}|\hat{\mathbf{j}}_x|\mathbf{x}\rangle . \quad (2.15)$$

In (2.15), $\hat{\mathbf{j}}_x$ must be the operator for current density explicitly associated with the density operator $\hat{\rho}$. To define $\hat{\mathbf{j}}_x$, first recall the classical current-density variable associated with a classical density f^c,

$$\mathbf{j}_x^c=f^c(\mathbf{p},\mathbf{q},t)\frac{d\mathbf{q}^c}{dt} . \quad (2.16)$$

The ensemble density $f^c(\mathbf{p},\mathbf{q},t)$ evolves in time, while the velocity is associated with a static phase-space point, i.e., $d\mathbf{q}^c/dt=\partial H/\partial\mathbf{p}$. If the factor ordering problem is resolved by symmetrization, then (2.16) may be quantized as

$$\hat{\mathbf{j}}_x(t)=\frac{1}{2}\left[\hat{\rho}(t)\frac{d\hat{\mathbf{x}}}{dt}+\frac{d\hat{\mathbf{x}}}{dt}\hat{\rho}(t)\right], \quad (2.17)$$

where $d\hat{\mathbf{x}}/dt$ equals $\hat{\mathbf{P}}/m$ for the Hamiltonian (2.2). Here $\hat{\mathbf{j}}_x(t)$ and $\hat{\rho}(t)$ are the Schrödinger picture operators in that the state of the system [i.e., $\hat{\rho}(t)$] evolves in time but $d\hat{\mathbf{x}}/dt$ is the time-independent expression $[\hat{H},\hat{\mathbf{x}}]/i\hbar$. The expression (2.17) appears somewhat unorthodox since it incorporates the density operator explicitly. The more usual procedure would be to formulate an operator independent of the state of the system which is then traced with the density operator. However, it may be easily verified that the approaches yield the same flux density. Specifically, if one employs the familiar point current operator $\hat{\mathbf{j}}(\mathbf{x})$,[71]

$$\hat{\mathbf{j}}(\mathbf{x})=\frac{1}{2}\left[|\mathbf{x}\rangle\langle\mathbf{x}|\frac{d\hat{\mathbf{x}}}{dt}+\frac{d\hat{\mathbf{x}}}{dt}|\mathbf{x}\rangle\langle\mathbf{x}|\right], \tag{2.18}$$

one can show

$$\mathrm{Tr}[\hat{\mathbf{j}}(\mathbf{x})\hat{\rho}]=\langle\mathbf{x}|\hat{\mathbf{j}}_x|\mathbf{x}\rangle . \tag{2.19}$$

Clearly, if we use the pure-state density operator $\hat{\rho}=|\Psi\rangle\langle\Psi|$, then the probability and current densities from (2.13) and (2.15) agree with those obtained previously, Eqs. (2.6) and (2.7), respectively.

The Von Neumann equation leads naturally to the continuity equation. For the full hydrodynamic description we also need the Euler equation. Since Von Neumann's equation is equivalent to the Schrödinger-picture equation of motion for the operator $\hat{\rho}$, it is natural that we consider the analogous Schrödinger-operator equation for $\hat{\mathbf{j}}_x$. Thus we have

$$\frac{\partial\hat{\mathbf{j}}_x}{\partial t}=\frac{1}{2}\left[\frac{\partial\hat{\rho}(t)}{\partial t}\frac{d\hat{\mathbf{x}}}{dt}+\frac{d\hat{\mathbf{x}}}{dt}\frac{\partial\hat{\rho}(t)}{\partial t}\right]$$
$$=\frac{1}{2i\hbar}\left[[\hat{H},\hat{\rho}]\frac{d\hat{\mathbf{x}}}{dt}+\frac{d\hat{\mathbf{x}}}{dt}[\hat{H},\hat{\rho}]\right] . \tag{2.20}$$

The diagonal expectation value in configuration space of the operator equation (2.20) can be verified to yield, upon manipulation, an Euler equation (see Appendix). Thus the hydrodynamic analogy directly carries over to mixed states if we use Eqs. (2.13) and (2.14) to define the fluid density variables $(\rho_x,\mathbf{j}_x)$. Finally, note that if the density operator is expressed in its diagonal basis,

$$\hat{\rho}=\sum_k c_k|\chi_k\rangle\langle\chi_k|\equiv\sum_k c_k\hat{\rho}^k , \tag{2.21}$$

then flux operator takes the simple form

$$\hat{\mathbf{j}}_x=\sum_k c_k\left[\hat{\rho}^k(t)\frac{d\hat{\mathbf{x}}}{dt}+\frac{d\hat{\mathbf{x}}}{dt}\hat{\rho}^k(t)\right]\equiv\sum_k c_k\hat{\mathbf{j}}_x^k . \tag{2.22}$$

Therefore the densities are given by the equally simple expressions,

$$\rho_x(\mathbf{x},t)=\sum_k c_k\rho_x^k(\mathbf{x},t) \tag{2.23}$$

and

$$\mathbf{j}_x(\mathbf{x},t)=\sum_k c_k\mathbf{j}_x^k(\mathbf{x},t) . \tag{2.24}$$

As pointed out by Messiah,[72] even for the case of a pure state the current density is not uniquely defined from the Schrödinger equation. The root problem is the ambiguity of factor ordering in quantum mechanics. The usual expression (2.7) is obtained by reexpressing the Schrödinger equation as a continuity equation and identifying the current. However, any $\mathbf{j}'_x(\mathbf{x},t)\equiv\mathbf{j}_x(\mathbf{x},t)+\delta\mathbf{j}_x$ where $\nabla_x\cdot\delta\mathbf{j}_x=0$, satisfies the continuity equation equally well. Furthermore, if $\delta\mathbf{j}_x$ scales to zero as $\hbar\to0$, then $\mathbf{j}'_x(\mathbf{x},t)$ and $\mathbf{j}_x(\mathbf{x},t)$ coincide in the classical limit. Even though one might also impose other conditions on $\mathbf{j}'_x(\mathbf{x},t)$, e.g., appropriate transformation properties under Galilean transformations, the current density is nevertheless to some degree ambiguous. However, since $\nabla_x\cdot\mathbf{j}'_x(\mathbf{x},t)=\nabla_x\cdot\mathbf{j}_x(\mathbf{x},t)$, the flux out of any closed volume is well defined. Therefore if physical observables are always carefully formulated in terms of fluxes out of closed volumes or (relatedly) through infinite dividing surfaces, unambiguous results may be obtained.

C. Momentum-space analysis

It is also possible to define the hydrodynamic analogy for transport in momentum space. Proceeding as above, the diagonal expectation value of the Von Neumann equation with momentum eigenstates yields

$$\left\langle\mathbf{p}\left|\frac{\partial\hat{\rho}}{\partial t}\right|\mathbf{p}\right\rangle=\frac{1}{i\hbar}\langle\mathbf{p}|[\hat{H},\hat{\rho}]|\mathbf{p}\rangle$$
$$=\frac{1}{i\hbar}(\langle\mathbf{p}|\hat{V}\hat{\rho}|\mathbf{p}\rangle-\langle\mathbf{p}|\hat{\rho}\hat{V}|\mathbf{p}\rangle) . \tag{2.25}$$

The hydrodynamic picture follows if (2.25) can be recast as the momentum-space continuity equation

$$\frac{\partial\rho_p(\mathbf{p},t)}{\partial t}=-\nabla_p\cdot\mathbf{j}_p(\mathbf{p},t) , \tag{2.26}$$

with

$$\rho_p(\mathbf{p},t)=\langle\mathbf{p}|\hat{\rho}|\mathbf{p}\rangle . \tag{2.27}$$

Since we are not able to find an explicit momentum flux density in the existing literature, we formulated the following nonlocal expression:

$$\mathbf{j}_p(\mathbf{p},t)=\frac{1}{(2\pi\hbar)^N}\int d^Nx\int d^Ny\exp[i\mathbf{p}\cdot(\mathbf{y}-\mathbf{x})/\hbar]$$
$$\times\mathbf{K}(\mathbf{x},\mathbf{y})\rho(\mathbf{x},\mathbf{y},t) , \tag{2.28}$$

where the kernel $\mathbf{K}(\mathbf{x},\mathbf{y})$ must satisfy

$$V(\mathbf{y})-V(\mathbf{x})=(\mathbf{x}-\mathbf{y})\cdot\mathbf{K}(\mathbf{x},\mathbf{y}) .$$

In one dimension one simply has

$$K(x,y)=\frac{V(y)-V(x)}{x-y} . \tag{2.29}$$

For an N-dimensional space one finds, after considerable effort,

$$\mathbf{K}(\mathbf{x},\mathbf{y})=-\tfrac{1}{2}\int_0^1[\nabla V(\mathbf{w}+t\mathbf{z})+\nabla V(\mathbf{w}-t\mathbf{z})]dt , \tag{2.30}$$

where

$$w=\frac{\mathbf{x}+\mathbf{y}}{2},\quad z=\frac{\mathbf{x}-\mathbf{y}}{2} .$$

One may verify that this expression satisfies the momentum-space continuity equation (2.26). The momentum flux density may be defined as the momentum expectation of a nonlocal flux operator,

$$\mathbf{j}_p(\mathbf{p},t)=\langle\mathbf{p}|\hat{\mathbf{j}}_p|\mathbf{p}\rangle , \tag{2.31}$$

where $\hat{\mathbf{j}}_p$ is defined by

$$\hat{\mathbf{j}}_p=\int d^Nx\int d^Ny|\mathbf{x}\rangle[\mathbf{K}(\mathbf{x},\mathbf{y})\rho(\mathbf{x},\mathbf{y},t)]\langle\mathbf{y}| . \tag{2.32}$$

Thus, unlike the configuration space flux, one finds that the operator formed by symmetrization of the classical momentum flux expression,

$$\hat{\mathbf{j}}_p^{\text{sym}}=\frac{1}{2}\left[\hat{\rho}(t)\frac{d\hat{\mathbf{P}}}{dt}+\frac{d\hat{\mathbf{P}}}{dt}\hat{\rho}(t)\right], \tag{2.33}$$

is valid only for quadratic potentials. [Actually, Eq. (2.17) will also break down if $\hat{H}$ contains $\hat{\mathbf{P}}$ to order higher than 2.] The current density $\mathbf{j}_p(\mathbf{p},t)$ is subject to the same sort of ambiguity of definition as was $\mathbf{j}_x(\mathbf{x},t)$, viz., the addition of any divergenceless quantity $\delta\mathbf{j}_p$ yields a current which satisfies the continuity equation (2.26) equally well.

The second hydrodynamic equation, i.e., the Euler-type equation, may in principle be obtained by taking the diagonal expectation value in momentum space of the Schrödinger-picture equation of motion for the operator $\hat{\mathbf{j}}_p$. In practice, the resulting integro-differential equation is too complicated to be very useful, although a formal expression may be written. This presents no particular problems for us here since we do not make use of the Euler equation to solve for the dynamics. The densities will be computed directly from the exact quantum dynamics. It is the continuity equation that is the most crucial relation to establish since it justifies the hydrodynamic picture, even when the fluid flows under the influence of complicated nonlocal forces as it does here.

D. Hydrodynamic analogy in coherent-state space

The behavior of the probability density and flux is now considered in a quantum phase-space representation. In what follows, we carry out the analysis explicitly for the coherent-state representation, although one expects similar results in other quantum phase-space representations. In the coherent-state representation, states and operators are projected onto a basis set of coherent states $|\mathbf{p},\mathbf{q}\rangle$. The characteristics of coherent states have been very heavily studied, especially in the optics literature, and so here only a few of the main properties are stated.[38,40,49] The coherent states are normalized Gaussian wave packets centered at the parameter $(\mathbf{p},\mathbf{q})$ in "phase space," which are defined through the relation

$$\langle\mathbf{x}|\mathbf{p},\mathbf{q}\rangle=(\pi\sigma^2)^{-N/4}\exp[-(\mathbf{x}-\mathbf{q})^2/2\sigma^2+i\mathbf{p}\cdot(\mathbf{x}-\mathbf{q}/2)\hbar] \tag{2.34}$$

for all real $(\mathbf{p},\mathbf{q})$. The Gaussian-width parameter σ may be set at our own discretion and will ultimately determine the relative resolution in $\mathbf{p}$ space versus $\mathbf{q}$ space. (The formalism presented here may easily be generalized to allow a different σ for each degree of freedom.) The collection of coherent states taken over all of $2N$-dimensional parameter space $(\mathbf{p},\mathbf{q})$ forms an overcomplete basis set and satisfies the resolution of identity relation

$$\hat{I}=\frac{1}{(2\pi\hbar)^N}\int\int d^Np\,d^Nq\,|\mathbf{p},\mathbf{q}\rangle\langle\mathbf{p},\mathbf{q}| . \tag{2.35}$$

The overlap between coherent states is given by

$$\langle\mathbf{p}',\mathbf{q}'|\mathbf{p},\mathbf{q}\rangle=\exp[-\tfrac{1}{2}|\mathbf{z}-\mathbf{z}'|^2+i\,\mathrm{Im}(\mathbf{z}\cdot\mathbf{z}')] , \tag{2.36}$$

with

$$\mathbf{z}\equiv\frac{1}{\sqrt{2}}\left[\frac{\mathbf{q}}{\sigma}+\frac{i\sigma\mathbf{p}}{\hbar}\right] . \tag{2.37}$$

The magnitude of the overlap

$$|\langle\mathbf{p}',\mathbf{q}'|\mathbf{p},\mathbf{q}\rangle|^2=\exp(-|\mathbf{z}-\mathbf{z}'|^2) \tag{2.38}$$

is seen to fall rapidly for packets centered in different regions of phase space.

In analogy to Eqs. (2.13) and (2.27), we consider the non-negative phase-space density $\rho(\mathbf{p},\mathbf{q},t)$ obtained from the diagonal matrix element of $\hat{\rho}$ in coherent-state space,

$$\rho(\mathbf{p},\mathbf{q},t)=\langle\mathbf{p},\mathbf{q}|\hat{\rho}|\mathbf{p},\mathbf{q}\rangle . \tag{2.39}$$

We regard $\rho(\mathbf{p},\mathbf{q},t)$ as a quasiprobability distribution in quantum phase space. We use the qualifier "quasi" since it does not exhibit all the properties one normally expects of a true probability distribution. For example,

$$\int\rho(\mathbf{p},\mathbf{q},t)d^Np\neq\langle\mathbf{q}|\hat{\rho}|\mathbf{q}\rangle ,$$

and

$$\int\rho(\mathbf{p},\mathbf{q},t)d^Nq\neq\langle\mathbf{p}|\hat{\rho}|\mathbf{p}\rangle .$$

Of course, $\rho(\mathbf{p},\mathbf{q},t)$ defined by (2.39) is an exact quantum-mechanical expression and we propose no approximation in its computation. However, one would implicity make a semiclassical interpretation of the dynamics if $\rho(\mathbf{p},\mathbf{q},t)$ were used as a true probability density in the phase space.

The dynamical evolution of $\rho(\mathbf{p},\mathbf{q},t)$ is determined from the diagonal expectation of the Von Neumann equation in coherent-state space,

$$\left\langle\mathbf{p},\mathbf{q}\left|\frac{\partial\hat{\rho}}{\partial t}\right|\mathbf{p},\mathbf{q}\right\rangle=\frac{1}{i\hbar}\langle\mathbf{p},\mathbf{q}|[\hat{H},\hat{\rho}]|\mathbf{p},\mathbf{q}\rangle ,$$

which is

$$\frac{\partial\rho(\mathbf{p},\mathbf{q},t)}{\partial t}=\frac{1}{i\hbar}\left[\left\langle\mathbf{p},\mathbf{q}\left|\frac{\hat{\mathbf{P}}^2}{2m}\hat{\rho}\right|\mathbf{p},\mathbf{q}\right\rangle-\left\langle\mathbf{p},\mathbf{q}\left|\hat{\rho}\frac{\hat{\mathbf{P}}^2}{2m}\right|\mathbf{p},\mathbf{q}\right\rangle\right]+\frac{1}{i\hbar}(\langle\mathbf{p},\mathbf{q}|\hat{V}\hat{\rho}|\mathbf{p},\mathbf{q}\rangle-\langle\mathbf{p},\mathbf{q}|\hat{\rho}\hat{V}|\mathbf{p},\mathbf{q}\rangle) . \tag{2.40}$$

Employing the diagonal basis for $\hat{\rho}$, and using the results

$$\langle\mathbf{p},\mathbf{q}|\hat{\mathbf{P}}|\chi_k\rangle=\left[\frac{\hbar}{i}\nabla_q+\frac{\mathbf{p}}{2}\right]\langle\mathbf{p},\mathbf{q}|\chi_k\rangle \tag{2.41}$$

and

$$\langle\mathbf{p},\mathbf{q}|\hat{\mathbf{P}}^2|\chi_k\rangle=\left[\frac{\hbar}{i}\nabla_q+\frac{\mathbf{p}}{2}\right]\langle\mathbf{p},\mathbf{q}|\hat{\mathbf{P}}|\chi_k\rangle , \tag{2.42}$$

one may verify that the first bracketed term on the right-hand side of Eq. (2.40) becomes

$$\frac{-1}{2m}\nabla_q\cdot(\langle\mathbf{p},\mathbf{q}|\hat{\mathbf{P}}\hat{\rho}|\mathbf{p},\mathbf{q}\rangle+\langle\mathbf{p},\mathbf{q}|\hat{\rho}\hat{\mathbf{P}}|\mathbf{p},\mathbf{q}\rangle)\equiv-\nabla_q\cdot\mathbf{j}_q(\mathbf{p},\mathbf{q},t) , \tag{2.43}$$

where $\mathbf{j}_q(\mathbf{p},\mathbf{q},t)$ is the coherent-state expectation of the configuration-space flux operator $\hat{\mathbf{j}}_x$, Eq. (2.17), i.e.,

$$\mathbf{j}_q(\mathbf{p},\mathbf{q},t)\equiv\langle\mathbf{p},\mathbf{q}|\hat{\mathbf{j}}_x|\mathbf{p},\mathbf{q}\rangle=\frac{1}{(\pi\sigma^2)^{N/2}}\frac{\hbar}{2mi}\int d^N x\int d^N y(\exp\{-[(\mathbf{x}-\mathbf{q})^2+(\mathbf{y}-\mathbf{q})^2]/2\sigma^2\}$$
$$\times\exp[i\mathbf{p}\cdot(\mathbf{y}-\mathbf{x})/\hbar][\nabla_x\rho(\mathbf{x},\mathbf{y},t)-\nabla_y\rho(\mathbf{x},\mathbf{y},t)])\ . \quad (2.44)$$

In a similar way, one may show after some manipulation that the second bracketed term on the right-hand side of Eq. (2.40) is

$$\frac{1}{i\hbar}(\langle\mathbf{p},\mathbf{q}|\hat{V}\hat{\rho}|\mathbf{p},\mathbf{q}\rangle-\langle\mathbf{p},\mathbf{q}|\hat{\rho}\hat{V}|\mathbf{p},\mathbf{q}\rangle)=-\nabla_p\cdot\mathbf{j}_p(\mathbf{p},\mathbf{q},t)\ , \quad (2.45)$$

where

$$\mathbf{j}_p(\mathbf{p},\mathbf{q},t)\equiv\langle\mathbf{p},\mathbf{q}|\hat{\mathbf{j}}_p|\mathbf{p},\mathbf{q}\rangle\ . \quad (2.46)$$

One may obtain an integral representation of $\mathbf{j}_p(\mathbf{p},\mathbf{q},t)$ using the representation (2.32) for $\hat{\mathbf{j}}_p$, i.e.,

$$\mathbf{j}_p(\mathbf{p},\mathbf{q},t)=\int d^N x\int d^N y\langle\mathbf{p},\mathbf{q}|\mathbf{x}\rangle[\mathbf{K}(\mathbf{x},\mathbf{y})\rho(\mathbf{x},\mathbf{y},t)]\langle\mathbf{y}|\mathbf{p},\mathbf{q}\rangle\ , \quad (2.47)$$

or, more explicitly,

$$\mathbf{j}_p(\mathbf{p},\mathbf{q},t)=\frac{1}{(\pi\sigma^2)^{N/2}}\int d^N x\int d^N y(\exp\{-[(\mathbf{x}-\mathbf{q})^2+(\mathbf{y}-\mathbf{q})^2]/2\sigma^2\}\exp[i\mathbf{p}\cdot(\mathbf{y}-\mathbf{x})/\hbar]\mathbf{K}(\mathbf{x},\mathbf{y})\rho(\mathbf{x},\mathbf{y},t))\ . \quad (2.48)$$

Thus the Von Neumann equation becomes a phase-space continuity equation

$$\frac{\partial\rho(\mathbf{p},\mathbf{q},t)}{\partial t}=-\nabla_p\cdot\mathbf{j}_p(\mathbf{p},\mathbf{q},t)-\nabla_q\cdot\mathbf{j}_q(\mathbf{p},\mathbf{q},t)$$
$$\equiv-\nabla\cdot\mathbf{J}(\mathbf{p},\mathbf{q},t)\ , \quad (2.49)$$

where

$$\nabla\equiv(\nabla_p,\nabla_q),\quad \mathbf{J}(\mathbf{p},\mathbf{q},t)\equiv[\mathbf{j}_p(\mathbf{p},\mathbf{q},t),\mathbf{j}_q(\mathbf{p},\mathbf{q},t)]\ .$$

The continuity equation ensures that it is proper to regard $\rho(\mathbf{p},\mathbf{q},t)$ as an indestructible quasiprobability fluid in quantum phase space whose time dependence is driven by the current density $\mathbf{J}(\mathbf{p},\mathbf{q},t)$.

III. CHARACTERISTICS OF THE PHASE-SPACE HYDRODYNAMIC MODEL

In Sec. II, we introduced the basic formal elements for the hydrodynamic analogy in coherent-state space. The essential step in that analysis was the formulation of the phase-space flux density $\mathbf{J}$, which together with ρ, satisfies the phase-space continuity equation. In this section, we discuss the analogy in more detail with special emphasis on issues related to the numerical generation of the quantum phase-space structure. In Sec. III A, we analyze the general characteristic of the hydrodynamic picture. In this section we make a clear statement as to how we propose to use the hydrodynamic model in studying quantum phase-space structure. In Sec. III B, we bring out the limiting behavior of the theory as $\hbar\to 0$. In Sec. III C, we come back to the point, raised in Sec. II, that the flux density is ambiguous due to factor ordering of the flux operators. It is shown that this ambiguity may be exploited, in analogy to gauge invariance in field theory, to simplify the quantum phase-space structure without in any way changing the transport of the density ρ. Finally, in Sec. III D we analytically implement the phase-space hydrodynamic picture for the harmonic oscillator and the free particle.

A. Hydrodynamic method for transport in quantum phase space

Associated with any quantum density operator $\hat{\rho}$ is the coherent-state quasi-probability-density $\rho(\mathbf{p},\mathbf{q},t)=\langle\mathbf{p},\mathbf{q}|\hat{\rho}|\mathbf{p},\mathbf{q}\rangle$. The essence of the hydrodynamic model is that $\rho(\mathbf{p},\mathbf{q},t)$ is to be interpreted as the density for an indestructible continuous fluid flowing in a quantum phase space. The existence of the phase-space continuity equation justifies such a picture in broad terms. The advantage of this identification is that now many of the classical concepts of fluid dynamics may be used to study quantum dynamics. Here, we shall show that a few of the more elementary aspects of the analogy may be exploited for the study of quantum mechanics.

The flow of a classical fluid may be regarded from either the Lagrangian or Eulerian points of view. From the Lagrangian viewpoint, a moving fluid consists of a continuum of discrete particles, each of which propagates along its own "fluid trajectory" under the influence external and internal forces. The fluid trajectories can be used to define a set of time-dependent Lagrangian coordinates which distinguish one evolving particle from another. Specifically, for a phase-space fluid one writes a classical trajectory as a function of initial conditions as

$$\mathbf{p}=\mathbf{p}(\mathbf{p}_0,\mathbf{q}_0,t)\ ,$$
$$\mathbf{q}=\mathbf{q}(\mathbf{p}_0,\mathbf{q}_0,t)\ , \quad (3.1)$$

where $\mathbf{p}_0=\mathbf{p}(\mathbf{p}_0,\mathbf{q}_0,0)$ and $\mathbf{q}_0=\mathbf{q}(\mathbf{p}_0,\mathbf{q}_0,0)$. If $(\mathbf{p},\mathbf{q})$ are taken as the usual static phase-space variables, then $(\mathbf{p}_0,\mathbf{q}_0)$ comprise a set of time-dependent Lagrangian coordinates. In the Euler approach, hydrodynamic laws

are formulated as fluid field equations in a static coordinate system such as $(\mathbf{p},\mathbf{q})$. One may transform between the Euler and Lagrange pictures using Eqs. (3.1).

The Lagrangian approach provides a very natural perspective on the flow of the classical phase-space density $f(\mathbf{p},\mathbf{q},t)$. The fluid flow consists of a ensemble of noninteracting particles which move along classical trajectories in phase space. Along each trajectory, the density satisfies Liouville's equation $df/dt=0$, which is equivalent to the phase-space continuity equation. The Lagrangian viewpoint is also very illuminating for the quantum phase-space fluid. Here the view is that the evolution of the density $\rho(\mathbf{p},\mathbf{q},t)$ is due to the propagation of quantum trajectories in the quantum phase space. The quantum trajectories may be used to define a set of Lagrangian coordinates as above. However, we note two important differences between the classical and quantum phase-space fluids. First, the quantum fluid trajectories show deviations from classical trajectories of order $O(\hbar)$ and higher, see Sec. III B for details. Second, the density does not satisfy Liouville's theorem $d\rho/dt\neq 0$, but instead varies in time along quantum trajectories. The differences are very important in that they provide hydrodynamic interpretations of nonclassical effects.

In classical mechanics, the trajectories are obtained directly from Hamilton's equations. In quantum theory, the trajectories are not generated by Hamiltonian dynamics. However, as suggested in Sec. I, we may use a straightforward numerical scheme to obtain the orbits. We assume that the density $\rho(\mathbf{p},\mathbf{q},t)$ and the flux density $\mathbf{J}(\mathbf{p},\mathbf{q},t)$ are known to us. In practice, these are numerically computed using the expressions (2.39), (2.44), and (2.48) employing an accurate $\rho(\mathbf{x},\mathbf{x}',t)$ obtained, e.g., from a basis set calculation. Given this, we define a phase-space velocity field as

$$\mathbf{J}(\mathbf{p},\mathbf{q},t)=\mathbf{v}(\mathbf{p},\mathbf{q},t)\rho(\mathbf{p},\mathbf{q},t)\ . \tag{3.2}$$

Using the velocity field, we may obtain the Lagrangian trajectories which govern the evolution of the density as solutions to

$$\begin{aligned}\frac{d\mathbf{p}}{dt}&=\mathbf{v}_p(\mathbf{p},\mathbf{q},t)\ ,\\ \frac{d\mathbf{q}}{dt}&=\mathbf{v}_q(\mathbf{p},\mathbf{q},t)\ .\end{aligned} \tag{3.3}$$

The time variation of the density along the trajectory is measured by the convective derivative $D\rho/Dt$,

$$\frac{D\rho}{Dt}\equiv\frac{\partial\rho}{\partial t}+\mathbf{v}\cdot\nabla\rho\ . \tag{3.4}$$

Making use of the continuity equation, we find

$$\frac{D\rho}{Dt}=\rho\nabla\cdot\mathbf{v}\ . \tag{3.5}$$

Equation (3.5) allows us to write a formal expression for the density ρ as a function of time,

$$\rho(\mathbf{p}(t),\mathbf{q}(t),t)=\exp\left[\int_0^t\nabla\cdot\mathbf{v}(\mathbf{p}(t'),\mathbf{q}(t'),t')dt'\right]\times\rho(\mathbf{p}(0),\mathbf{q}(0),0) \tag{3.6}$$

where $\{\mathbf{p}(t),\mathbf{q}(t)\}$ is a fluid trajectory.

In classical mechanics the phase-space velocity field is divergenceless reflecting the Hamiltonian structure, or equivalently, the conservation of phase-space volume. Hence from (3.6) the classical density is conserved. In quantum phase space, $\nabla\cdot\mathbf{v}$ is usually nonzero, so there is an associated expansion or contraction of phase space along the flow, *Note that even for a stationary distribution, such as that from an energy eigenstate,* $\nabla\cdot\mathbf{J}=0$ *but generally* $\nabla\cdot\mathbf{v}\neq 0$.

The structure of quantum phase space corresponding to $\hat{\rho}$ may be determined using the first-order ODE's (3.3) as one uses classical trajectories in classical dynamics. As just mentioned, one important difference between the classical and quantum theories is that the quantum first-order flow is non-Hamiltonian, i.e., $\nabla\cdot\mathbf{v}\neq 0$. Another significant difference is that the quantum phase-space structure depends on the choice of initial $\hat{\rho}$ at order $O(\hbar)$ and higher. This is unlike the classical problem where the classical Hamiltonian determines the phase-space structure and any chosen ensemble $f(\mathbf{p},\mathbf{q},t)$ evolves according to that fixed structure. The quantum density behaves more like a typical liquid in this regard with the evolution of the Lagrangian fluid trajectories reflecting not only the influence of the external force $-\nabla V$, but also the density-dependent internal stresses. We emphasize that the $\hat{\rho}$ dependence of the phase-space structure is not an artifact of the method but is physically significant and provides insight into the dynamical differences exhibited by different states. For example, certain quantum symmetry constraints should be reflected in different phase-space structures for states of different symmetry.

In contrast to most previous treatments, we have not emphasized the role of the Euler equation in the hydrodynamic analogy. This is because in our approach the exact $\hat{\rho}$ is provided as input and the Euler equation is thus not required to solve for the densities. We pointed out that in principle, the Euler equation may be written as the diagonal expectation of the Schrödinger evolution equation for the flux operator. In practice, it seems that the resulting integro-differential equation will usually be very difficult to solve and there is no motivation to do so here.

B. Correspondence limit

One expects in the limit $\hbar\to 0$ that the quantum phase-space continuity equation should reduce to the classical Liouville equation and that the Lagrangian fluid trajectories should approach classical trajectories. In this section it is shown that this is the case and characteristics of the quantum corrections are discussed.

First, consider the relationship between the flux density $\mathbf{J}$ and the quasi-probability-density ρ. Using the result

$$\langle\mathbf{p},\mathbf{q}|\hat{\mathbf{P}}|\chi_k\rangle=\left[\mathbf{p}-\frac{\hbar\mathbf{q}}{2i\sigma^2}+\frac{\hbar^2}{\sigma^2}\nabla_p\right]\langle\mathbf{p},\mathbf{q}|\chi_k\rangle \tag{3.7}$$

in the diagonal representation of $\hat{\rho}$, it is easy to show that

$$\mathbf{j}_q(\mathbf{p},\mathbf{q},t)=\frac{\mathbf{p}}{m}\rho+\frac{\hbar^2}{2m\sigma^2}\nabla_p\rho\ . \tag{3.8}$$

The first term on the right-hand side of Eq. (3.8) is the classical result, while the second term is a quantum correction. The relationship between $\mathbf{j}_p$ and ρ can also be found. Begin by expanding the integral kernel $\mathbf{K}(\mathbf{x},\mathbf{y})$ of $\mathbf{j}_p$ in a Taylor expansion in both $\mathbf{x}$ and $\mathbf{y}$ about the point $\mathbf{q}$, the center of the Gaussian, to obtain

$$\mathbf{K}(\mathbf{x},\mathbf{y})=-\nabla_q V(\mathbf{q})-\tfrac{1}{2}\frac{\partial\nabla_q V(\mathbf{q})}{\partial q_i}(\Delta x_i+\Delta y_i) -\frac{1}{6}\frac{\partial^2\nabla_q V(\mathbf{q})}{\partial q_i\partial q_j}(\Delta x_i\Delta x_j+\Delta x_i\Delta y_j+\Delta y_i\Delta y_j) +\cdots , \tag{3.9}$$

where

$$\Delta x_i=x_i-q_i,\quad \Delta y_i=y_i-q_i ,$$

and repeated index summations is assumed. Inserting this expansion into Eq. (2.48) one obtains for $\mathbf{j}_p(\mathbf{p},\mathbf{q},t)$,

$$\mathbf{j}_p(\mathbf{p},\mathbf{q},t)=-\rho\nabla_q V(\mathbf{q})-\frac{\sigma^2}{2}\frac{\partial\nabla_q V(\mathbf{q})}{\partial q_i}\frac{\partial\rho}{\partial q_i} -\frac{1}{6}\frac{\partial^2\nabla_q V(\mathbf{q})}{\partial q_i\partial q_j}\left[\frac{3\sigma^4}{4}\frac{\partial^2\rho}{\partial q_i\partial q_j}-\frac{\hbar^2}{4}\frac{\partial^2\rho}{\partial p_i\partial p_j} +\tfrac{3}{2}\delta_{ij}\sigma^2\rho\right]+\cdots . \tag{3.10}$$

The first term is the classical momentum flux $\rho\dot{\mathbf{p}}$ and the remaining terms are quantum-mechanical corrections.

The quantum scaling properties of the correction terms to $\mathbf{J}$ depend on the $\hbar$ dependence of the width parameter σ. Clearly, from the Gaussian form of the coherent state, σ is roughly the resolution in configuration space Δq. The resolution in momentum space is $\Delta p\sim\hbar/\sigma$. Thus, if one varies $\hbar$ in such a way as to maintain a constant ratio $\Delta p/\Delta q$, then σ should scale to zero as $\hbar^{1/2}$ in the classical limit. In what follows, we imagine that the classical limit is approached in such a fashion.

The quantum phase-space continuity equation can be rewritten as

$$\frac{\partial\rho}{\partial t}=-\frac{\mathbf{p}}{m}\nabla_q\rho+\nabla_p\rho\cdot\nabla_q V(\mathbf{q})-\left[\frac{\hbar^2}{2m\sigma^2}\nabla_q\cdot\nabla_p\rho-\frac{\sigma^2}{2}\frac{\partial\nabla_q V(\mathbf{q})}{\partial q_i}\cdot\frac{\partial\nabla_p\rho}{\partial q_i}-\frac{\delta_{ij}\sigma^2}{4}\frac{\partial^2\nabla_q V(\mathbf{q})}{\partial q_i\partial q_j}\cdot\nabla_p\rho\right] +\frac{1}{6}\frac{\partial^2\nabla_q V(\mathbf{q})}{\partial q_i\partial q_j}\cdot\left[\frac{3\sigma^4}{4}\frac{\partial^2\nabla_p\rho}{\partial q_i\partial q_j}-\frac{\hbar^2}{4}\frac{\partial^2\nabla_p\rho}{\partial p_i\partial p_j}\right]+\cdots=\{H^{cl},\rho\}_{\mathrm{PB}}+O(\hbar)+O(\hbar^2)+\cdots . \tag{3.11}$$

Thus one obtains the classical Liouville equation plus quantum correction terms which scale to zero as $\hbar\to 0$. In fact, by eliminating $\mathbf{J}$ in favor of ρ in this way we begin to develop the infinite-order quantum Liouville equation discussed previously by, e.g., Prugovecki[43] and Takahashi.[22]

In a similar way, using Eqs. (3.8) and (3.10), the trajectory equations can be expressed as

$$\frac{d\mathbf{p}}{dt}=-\nabla_q V(\mathbf{q})+O(\hbar)+O(\hbar^2)+\cdots ,\qquad \frac{d\mathbf{q}}{dt}=\frac{\mathbf{p}}{m}+O(\hbar) , \tag{3.12}$$

which are Hamilton's equations plus quantum corrections of leading order $O(\hbar)$.

Finally, we note that caution is required in making $\hbar$ expansions of the quantum phase-space dynamics. As emphasized by Tatarskii,[45] and others,[41,42] there may be implicit $\hbar$ dependence in ρ due to quantum initial conditions in addition to the explicit $\hbar$ dependence in the equations of motion such as that considered above. Equations (3.11) and (3.12) are appropriate if this $\hbar$ dependence of ρ is ignored.

C. Flux gauge

In Sec. II, we pointed out that the flux densities were not uniquely defined in quantum mechanics due to factor ordering ambiguities in the definition of the flux operators. Effectively, one may add a divergenceless single-valued vector function to the flux density,

$$\mathbf{J}'\equiv\mathbf{J}+\delta\mathbf{J} , \tag{3.13}$$

where $\delta\mathbf{J}\to 0$ as $\hbar\to 0$, and still maintain an expression which satisfies the continuity equation and the correspondence principle. Thus the transport of the density ρ is equally well explained by any $\mathbf{J}'$ defined by (3.13), since the net flux out of any closed volume of phase space is the same.

In the configuration-space analysis, there has been little reason to question the usual expression for flux density, Eq. (2.7), except for a straightforward generalization to vector potentials. On the other hand, in the present phase-space context, an appropriate choice of $\delta\mathbf{J}$ may greatly simplify the task of resolving the quantum phase-space structure. For example, $\delta\mathbf{J}$ may be chosen to eliminate small (on the scale of Planck's constant) eddies and whirlpools in $\mathbf{J}$ which complicate the phase-space structure but ultimately do not influence transport. Thus the term $\delta\mathbf{J}$ has a similar character to a gauge factor in field theory and we henceforth refer to the specification of $\mathbf{J}$ as the choice of flux gauge.

One can imagine any number of flux gauges that could prove useful in simplifying various problems. Here, we explicitly consider only two possible choices. First, the simplest flux gauge is where $\delta\mathbf{J}=0$ so that one uses directly the diagonal coherent state expectation of the flux operators Eqs. (2.24) and (2.48). We shall call this

choice the "primitive gauge." A second gauge is

$$\delta\mathbf{J}=\frac{\hbar^2}{2m\sigma^2}(\nabla_q\rho,-\nabla_p\rho)\ , \tag{3.14}$$

which is chosen to eliminate the quantum correction term to $\mathbf{j}_q$ in Eq. (3.8). Thus we shall refer to (3.14) as the "classical gauge." Using the classical gauge, the q-space velocity becomes $\mathbf{v}_q=\mathbf{p}/m$, which means that any stagnation points of the fluid, $\mathbf{v}=\mathbf{0}$, must lie at $\mathbf{p}=\mathbf{0}$, which is intuitively preferred.

Finally, an intriguing, if somewhat speculative, possibility is that the flux gauge may be set to make the quantum dynamics resemble a classical Hamiltonian system. That is, we can imagine choosing $\delta\mathbf{J}$ to make the velocity field divergenceless. Specifically, if we define $\delta\mathbf{J}=\rho\delta\mathbf{v}$ and $\mathbf{v}'=\mathbf{v}+\delta\mathbf{v}$, then we select $\delta\mathbf{v}$ to enforce $\nabla\cdot\delta\mathbf{J}=0$ and $\nabla\cdot\mathbf{v}'=0$. For a static distribution $\partial\rho/\partial t=0$, this implies that the trajectories will lie along equidensity contours of ρ. For nonstationary distribution, the fluid orbits should correspond to the Hamiltonian trajectories of some time-dependent Hamiltonian $K(\mathbf{p},\mathbf{q},t)$. Although we shall not use this "Hamiltonian" gauge in this work, it clearly warrants further investigation.

D. Analytic examples

In order to illustrate the phase-space hydrodynamic model and see the effects of the flux gauge, we consider two simple analytically solvable problems: the free particle and the harmonic oscillator.

1. The free particle

Consider first a plane-wave state for a free particle of mass m in three space $|\mathbf{p}'\rangle$. The density is easily found to be

$$\begin{aligned}\rho(\mathbf{p},\mathbf{q},t)&=|\langle\mathbf{p},\mathbf{q}|\mathbf{p}'\rangle|^2\\&=\frac{\sigma^2}{(\pi\hbar^2)^{3/2}}\exp[-(\mathbf{p}-\mathbf{p}')^2\sigma^2/\hbar^2]\ .\end{aligned} \tag{3.15}$$

Using the gauge $\delta\mathbf{J}=0$, we find the current and velocity fields

$$\mathbf{J}=\left[0,\frac{\mathbf{p}'}{m}\right]\rho,\quad \mathbf{v}=\left[0,\frac{\mathbf{p}'}{m}\right]\ . \tag{3.16}$$

Thus the entire quantum phase space $(\mathbf{p},\mathbf{q})$ has a constant velocity $(0,\mathbf{p}'/m)$ determined by the momentum of the plane wave. On the other hand, the same problem may be solved in the classical gauge, (3.14). The density ρ, of course, does not change, but flux and velocity fields become

$$\mathbf{J}=\left[0,\frac{\mathbf{p}}{m}\right]\rho,\quad \mathbf{v}=\left[0,\frac{\mathbf{p}}{m}\right]\ . \tag{3.17}$$

Thus the velocity field becomes exactly the same as that of a classical free particle $(-\nabla_q H,\nabla_p H)=(0,\mathbf{p}/m)$ independent of $\mathbf{p}'$. Obviously, the two descriptions are the same at $\mathbf{p}=\mathbf{p}'$, where density is peaked. In physical terms, of course, one is mainly interested in regions of phase space where the density and flux are highest. Hence, while the two cases $\mathbf{v}=(0,\mathbf{p}'/m)$ and $\mathbf{v}=(0,\mathbf{p}/m)$ may differ by arbitrarily large amounts when $|\mathbf{p}-\mathbf{p}'|$ is increased, meaningful differences are bounded by the range of ρ (and hence $\mathbf{J}$) $\Delta p\sim\hbar/\sigma$. When the effects of range are taken into account, the differences between the dynamical descriptions afforded by the two gauges scale to zero as $\hbar\to0$, even though the velocity fields do not show an apparent $\hbar$ dependence.

It is also interesting to consider the same three-dimensional free particle, but now described by the Boltzmann density operator $\hat{\rho}=\exp(-\beta\hat{H})$ where $\beta\equiv1/kT$. Straightforward integration yields the corresponding coherent-state density,

$$\rho(\mathbf{p},\mathbf{q},t)=(1+y)^{-3/2}\exp\left[\frac{-\beta\mathbf{p}^2}{2m}\frac{1}{1+y}\right]\ , \tag{3.18}$$

where y is the energy dispersion of a coherent-state packet of width σ measured in units of kT, i.e., $y=\beta\hbar^2/2m\sigma^2$. Note that in the high-temperature limit $y\to0$, ρ approaches the classical Boltzmann distribution. At low temperatures, ρ approaches a limiting Gaussian corresponding to the energy spread determined by the width σ,

$$\rho(\mathbf{p},\mathbf{q},t)\to(1+y)^{-3/2}\exp\left[\frac{-\mathbf{p}^2\sigma^2}{\hbar^2}\right]\ . \tag{3.19}$$

In the primitive gauge $\delta\mathbf{J}=0$, the flux and velocity fields are given by

$$\begin{aligned}\mathbf{J}&=\left[0,\frac{\mathbf{p}}{m}\left[1-\frac{y}{2(1+y)}\right]\right]\rho\ ,\\ \mathbf{v}&=\left[0,\frac{\mathbf{p}}{m}\left[1-\frac{y}{2(1+y)}\right]\right]\ .\end{aligned} \tag{3.20}$$

Thus at high temperatures the phase-space structure is equivalent to the classical free particle but, at low temperatures, temperature-dependent quantum corrections appear. Using the classical gauge, Eq. (3.14), the vector fields are given by

$$\mathbf{J}=\left[0,\frac{\mathbf{p}}{m}\right]\rho,\quad \mathbf{v}=\left[0,\frac{\mathbf{p}}{m}\right]\ , \tag{3.21}$$

which gives the classical phase-space structure at all temperatures. Note that both choices of gauge yield stagnation of the quantum fluid only along the hyperplane $\mathbf{p}=0$.

Finally, as an example of a time-dependent free particle, we consider a one-degree-of-freedom particle which evolves as a pure-state normalized Gaussian packet

$$\Psi(x,t)=\left[\frac{\pi}{2\alpha_R}\right]^{-1/4}\exp[-\alpha(x-q_t)^2+ip_t(x-q_t)/\hbar+i\gamma/\hbar]\ , \tag{3.22}$$

where (p_t,x_t) is any classical trajectory for the free particle,

$$p_t=\text{const},\quad q_t=\frac{p_t}{m}t+q_0\ , \tag{3.23}$$

and the other parameters are

$$\alpha=\frac{\alpha_0}{1+2i\hbar^2\alpha_0 t/m}\ ,$$
$$\gamma=\frac{\hbar^2}{m}\int_0^t\alpha_R\,dt'+\frac{p_t^2}{2m}\ , \tag{3.24}$$

with $\alpha\equiv\alpha_R+i\alpha_I$ and $\alpha_0=\alpha(t=0)$. The coherent-state density is found to be

$$\rho(p,q,t)=N\exp[-A(q-q_t)^2-B(p-p_t)^2 -C(q-x_t)(p-p_t)]\ , \tag{3.25}$$

where

$$A=\text{Re}\frac{2\alpha}{1+2\sigma^2\alpha},\quad B=\frac{\sigma^2}{\hbar^2}\text{Re}\frac{1}{1+2\sigma^2\alpha}\ ,$$
$$C=\frac{1}{\hbar}\text{Im}\frac{2}{1+2\sigma^2\alpha}\ , \tag{3.26}$$

and N is the normalization factor. Thus the coherent-state distribution is a Gaussian in phase space centered on the evolving classical trajectory (p_t,q_t). The width of the distribution varies with time and is a composition of the natural width α and the coherent-state width σ. For very long times the wave packet will always spread in configuration space, since, as $t\to\infty$, $\alpha_R\to 0$, at order $O(t^{-2})$, and $\alpha_I\to 0$, order $O(t^{-1})$. The coherent-state density also spreads in the q direction, since $A\to 0$, $O(t^{-2})$. The phase-space skewing term $C(q-x_t)(p-p_t)$ also falls away since $C\to 0$, $O(t^{-1})$. However, the distribution along the p direction approaches a limiting form since $B\to\sigma^2/\hbar^2$ as $t\to\infty$, and in fact approaches the expression for a plane wave of momentum p_t, as one should expect. On the other hand, if the wave packet is made exceedingly narrow at some initial time, so that α_R is very large, then $A\to 1/\sigma^2$ while $B\to 0$ and $C\to 0$. Hence the coherent-state density is as narrow as it can be made in the q direction given the coherent-state width itself, viz., $A=1/\sigma^2$, but is completely delocalized in the p direction.

Now, in the gauge $\delta\mathbf{J}=0$, the flux and velocity fields are

$$\mathbf{J}=\left[0,\text{Re}\frac{p_t+2\sigma^2\alpha p}{m(1+2\sigma^2\alpha)}-\text{Im}\frac{\hbar(q-q_t)}{m\sigma^2(1+2\sigma^2\alpha)}\right]\rho \tag{3.27}$$

and

$$\mathbf{v}=\left[0,\text{Re}\frac{p_t+2\sigma^2\alpha p}{m(1+2\sigma^2\alpha)}-\text{Im}\frac{\hbar(q-q_t)}{m\sigma^2(1+2\sigma^2\alpha)}\right]\ . \tag{3.28}$$

Unlike previous examples, the velocity field depends on q. This reflects the frequency modulation in the wave packet due to the imaginary part of the width parameter α. When $\alpha_I=0$ the q dependence in $\mathbf{v}$ disappears. At the center of the distribution, $(p,q)=(p_t,q_t)$, the velocity field assumes the classical value $\mathbf{v}(p_t,q_t)=(0,p_t/m)$. Away from the center, there are quantum corrections which depend on the width parameter α. In the limit of very narrow wave packets, $\alpha_R\to\infty$, the velocity field approaches $\mathbf{v}=(0,p/m)$, the classical result, over the entire phase space. On the other hand, for very wide wave packets, the velocity field approaches $(0,p_t/m)$, so the whole quantum phase space has the constant velocity of the center of the packet, as happened for the plane-wave state. If the problem is expressed in the classical gauge, (3.14), the expressions become

$$\mathbf{J}(p,q,t)=\left[\frac{-\hbar^2}{m\sigma^2}\left[\text{Re}\frac{2\alpha(q-q_t)}{1+2\sigma^2\alpha}+\frac{1}{\hbar}\text{Im}\frac{(p-p_t)}{1+2\sigma^2\alpha}\right],\frac{p}{m}\right]\rho \tag{3.29}$$

and

$$\mathbf{v}(p,q,t)=\left[\frac{-\hbar^2}{m\sigma^2}\left[\text{Re}\frac{2\alpha(q-q_t)}{1+2\sigma^2\alpha}+\frac{1}{\hbar}\text{Im}\frac{(p-p_t)}{1+2\sigma^2\alpha}\right],\frac{p}{m}\right]\ . \tag{3.30}$$

The q component of the velocity field is the classical velocity p/m everywhere in phase space. The price paid for this is that, for the first time, the velocity vector field has acquired a nonzero p component. However, at the center of the distribution, $(p,q)=(p_t,q_t)$, the p component is zero and the velocity field is the classical result $(0,p_t/m)$. Furthermore, even though $J_p\neq 0$, there is no net transport in momentum space. That is, if we calculate the total flux through the infinite surface $p=p_0$, we find

$$\int_{-\infty}^{\infty}J_p\,dq=\frac{\hbar^2}{2m\sigma^2}\int_{-\infty}^{\infty}\frac{\partial\rho}{\partial q}dq$$
$$=\frac{\hbar^2}{2m\sigma^2}[\rho(p_0,q=\infty)-\rho(p_0,q=-\infty)]$$
$$=0\ , \tag{3.31}$$

which holds at every instant. The flux gauge merely introduces a circulation in phase space but with no net momentum transport as would occur with a nonzero potential.

2. *The harmonic oscillator*

Next, we consider the dynamics of a harmonic oscillator of frequency ω. We first analyze the motion of a coherent-state wave packet. The time-dependent wave function is

$$\Psi(x,t)=(\pi\sigma^2)^{-1/4}\exp[-(x-q_t)^2/2\sigma^2 + ip_t(x-q_t/2)/\hbar - i\omega t/2] , \tag{3.32}$$

where $\sigma^2=\hbar/m\omega$ and (p_t,q_t) is a classical trajectory

$$(p_t,q_t)=[(2mE)^{1/2}\cos(\omega t+\theta_0) , (2E/m\omega^2)^{1/2}\sin(\omega t+\theta_0)] . \tag{3.33}$$

Employing the same width parameter σ, the coherent-state density corresponding to $\hat{\rho}=|\Psi\rangle\langle\Psi|$ is

$$\rho(p,q,t)=\exp[-(q-q_t)^2/2\sigma^2-(p-p_t)^2\sigma^2/2\hbar^2] . \tag{3.34}$$

This is a rigid Gaussian distribution whose center evolves along the classical orbit. In the $\delta\mathbf{J}=0$ gauge, the flux density is easily found to be

$$\mathbf{J}(p,q,t)=\left[\frac{-m\omega^2(q+q_t)}{2},\frac{p+p_t}{2m}\right]\rho(p,q,t) , \tag{3.35}$$

and the associated velocity field is

$$\mathbf{v}(p,q,t)=\left[\frac{-m\omega^2(q+q_t)}{2},\frac{p+p_t}{2m}\right] . \tag{3.36}$$

The velocity field is thus the average of the static classical velocity field $\mathbf{v}_c=(-m\omega^2q,p/m)$ and the uniform, but time-dependent, velocity of the center of the packet $\mathbf{v}_t=(-m\omega^2q_t,p_t/m)$, i.e., $\mathbf{v}=(\mathbf{v}_c+\mathbf{v}_t)/2$. The phase point at the center of the wave packet, $(p,q)=(p_t,q_t)$, exhibits the classical velocity with $\mathbf{v}=\mathbf{v}_c=\mathbf{v}_t$. We emphasize again that while $\mathbf{v}$ appears to show deviations from the classical result of order $O(\hbar^0)$, if we restrict our attention to the region of phase space bounded by the range of ρ, the quantum effects do scale to zero in the classical limit. If we use, instead, the classical gauge Eq. (3.14), we find that flux and velocity fields become identical to the classical results

$$\mathbf{J}(p,q,t)=(-m\omega^2q,p/m)\rho(p,q,t) , \quad \mathbf{v}(p,q,t)=(-m\omega^2q,p/m) . \tag{3.37}$$

Thus in this gauge, the wave packet propagates as each element of the density ρ evolves along its own classical trajectory. Specifically, since $\nabla\cdot\mathbf{v}=0$, Eq. (3.6) implies that $\rho(p_t,q_t,t)=\rho(p_0,q_0,0)$, which is classical Liouville propagation of the density.

Next, consider the same harmonic-oscillator system but in an eigenstate $|n\rangle$ of the Hamiltonian. Using the well-known result

$$|p,q\rangle=\exp(-|z|^2/2)\sum_{n=0}^{\infty}\frac{z^n}{(n!)^{1/2}}|n\rangle , \tag{3.38}$$

where $z=(q/\sigma+i\sigma p/\hbar)/\sqrt{2}$, we obtain for the coherent-state density

$$\rho(p,q,t)=\exp(-\epsilon)\frac{\epsilon^n}{n!} , \tag{3.39}$$

with

$$\epsilon=|z|^2=\frac{1}{\hbar\omega}\left[\frac{p^2}{2m}+\frac{1}{2}m\omega^2q^2\right] . \tag{3.40}$$

This is a static distribution which is peaked on the circle $\epsilon=n$, which is located near the corresponding EBK orbit at $\epsilon=n+1/2$. When the gauge is set with $\delta\mathbf{J}=0$, the static flux and velocity fields are found to be

$$\mathbf{J}(p,q,t)=(-m\omega^2q,p/m)[1+\tfrac{1}{2}(n/\epsilon-1)]\rho(p,q,t) \tag{3.41}$$

and

$$\mathbf{v}(p,q,t)=(-m\omega^2q,p/m)[1+\tfrac{1}{2}(n/\epsilon-1)] . \tag{3.42}$$

The bracketed term is unity on the circle $\epsilon=n$ and therefore the fields assume their classical value on that curve. If the gauge is instead chosen as (3.14) then the fields reduce to the classical expressions everywhere in phase space

$$\mathbf{J}(p,q,t)=(-m\omega^2q,p/m)\rho(p,q,t) , \quad \mathbf{v}(p,q,t)=(-m\omega^2q,p/m) . \tag{3.43}$$

Finally, we consider the coherent-state analysis for the canonical ensemble $\hat{\rho}=\exp(-\beta\hat{H})$. Performing a Boltzmann average of Eq. (3.39), we easily find for the coherent-state density

$$\rho(p,q,t)=\exp[-\epsilon(1-e^{-\lambda})-\lambda/2] , \tag{3.44}$$

where $\lambda\equiv\beta\hbar\omega$ and ϵ is classical Hamiltonian divided by $\hbar\omega$, Eq. (3.40). In the high-temperature limit $\lambda\to0$, $\rho(p,q,t)$ is seen to go to the classical Boltzmann distribution $\exp(-\epsilon\lambda)$. At low temperatures $\lambda\to\infty$, $\rho(p,q,t)$ becomes the coherent-state density for the ground state $\exp(-\epsilon)$ times the ground-state Boltzmann factor. In the gauge $\delta\mathbf{J}=0$, the temperature-dependent flux and velocity fields are found to be

$$\mathbf{J}(p,q,t)=(-m\omega^2q,p/m)[1+\tfrac{1}{2}(e^{-\lambda}-1)]\rho(p,q,t) \tag{3.45}$$

and

$$\mathbf{v}(\rho,q,t)=(-m\omega^2q,p/m)[1+\tfrac{1}{2}(e^{-\lambda}-1)] . \tag{3.46}$$

With the gauge (3.14), $\mathbf{J}$ and $\mathbf{v}$ again become the temperature-independent classical harmonic-oscillator fields, Eqs. (3.43).

IV. NONLINEAR PHASE-SPACE STRUCTURE OF STATES IN A DOUBLE WELL

In Sec. III, the phase-space hydrodynamic model was implemented analytically for the simple cases of the harmonic oscillator and the free particle. In this section, we consider a more complicated problem which is not analytic and which shows nonlinear quantum phase-space structure, viz., the quartic double-well problem. We use this application to illustrate several general techniques to

numerically resolve nonlinear structures using the fluid trajectories. Specifically, the role of fixed points and separatrix structure are found to be especially important. We shall emphasize the description of the tunneling phenomena in this system in order to illustrate how nonclassical effects can be interpreted using the quantum phase-space structure.

We consider the time-dependent quantum dynamics for the quartic double-well problem governed by the Hamiltonian

$$\hat{H}=\frac{\hat{\mathbf{P}}^2}{2}-\frac{\hat{\mathbf{q}}^2}{2}+\gamma\hat{\mathbf{q}}^4 . \tag{4.1}$$

The value of the parameter γ determines the number of states trapped below the barrier. Since in this paper we are interested particularly in nonclassical manifestations in quantum phase space, we set $\gamma=\frac{3}{100}$, which yields only four states with energy below the barrier, see Fig. 1. We specifically consider time-dependent pure states which are linear combinations of neighboring pairs of symmetric (+) and antisymmetric (−) eigenstates

$$|\Psi\rangle=\frac{1}{\sqrt{2}}(|E_j^+\rangle e^{-iE_jt/\hbar A}+|E_{j+1}^-\rangle e^{-iE_{j+1}t/\hbar}) . \tag{4.2}$$

For energies less than zero, the barrier energy, the transport is due to a tunneling process. The period for a tunneling cycle is given by

$$\tau_{\text{tun}}=\frac{h}{E_{j+1}-E_j} . \tag{4.3}$$

The goal in this study is to resolve the quantum phase-space structures responsible for the tunneling and to demonstrate that the tunneling rates may be computed directly based on the phase-space structure.

The energy eigenstates for this system were found by numerically diagonalizing the Hamiltonian in a large basis set. The density ρ and the flux density $\mathbf{J}$ were then obtained by numerical integration using the defining expressions, Eqs. (2.39), (2.44), and (2.48). The flux gauge was chosen as Eq. (3.14), which simplifies the q component of the flux to $J_q=\rho p/m$. One feature of this gauge which is particularly useful is that the instantaneous fixed points, where $\mathbf{v}=\mathbf{0}$, must now be constrained to lie on the $p=0$ axis. This simplifies the overall phase-space structure by eliminating certain small quantum eddies off the $p=0$ axis which do not contribute to the net transport. Furthermore, locating the fixed points in this gauge simplifies to a one-dimensional search.

In Fig. 3, the influence of the choice of flux gauge is brought out for the superposition of the lowest pair of eigenstates via Eq. (4.2). At the time $t=\tau_{\text{tun}}/5$, a representative set of streamline trajectories is plotted for the gauge $\delta\mathbf{J}=\mathbf{0}$, in the upper panel, and the gauge (3.14) in the lower panel. It is gratifying to see that the overall structure of the quantum phase space is not greatly affected by the gauge. However, the small eddy lying above the x point is eliminated by the gauge (3.14). The significance of the various other phase-space structures revealed in Fig. 3 will be discussed below.

The dynamics of the time-dependent wave packet is represented by a first-order flow in a three-dimensional quantum phase space,

$$\frac{dp}{dt}=v_p(p,q,\tau) , \tag{4.4a}$$

$$\frac{dq}{dt}=v_q(p,q,\tau) , \tag{4.4b}$$

$$\frac{d\tau}{dt}=1 . \tag{4.4c}$$

Such first-order systems have been much studied and will, in general, exhibit a rich variety of generic nonlinear dynamics.[69] One way to depict the resulting phase-space structure is using a discrete map where, e.g., (p,q) is plotted for the regularly spaced times $\tau=n\tau_{\text{tun}}$. Alternatively, when the explicit time variation of $\mathbf{v}$ is very slow compared to the typical orbit period, one may interpret the dynamics using the continuous two-dimensional orbits of the instantaneous flow. The instantaneous flow is the result of holding τ fixed on the right-hand side of Eqs. (4.4a) and (4.4b) so that the resulting orbits are the streamlines for the instantaneous velocity field. While the discrete map may be the more generally applicable representation, we adopt the second approach for our specific problem here since it will yield more insight into the dynamics. For the pairs of states considered, the tun-

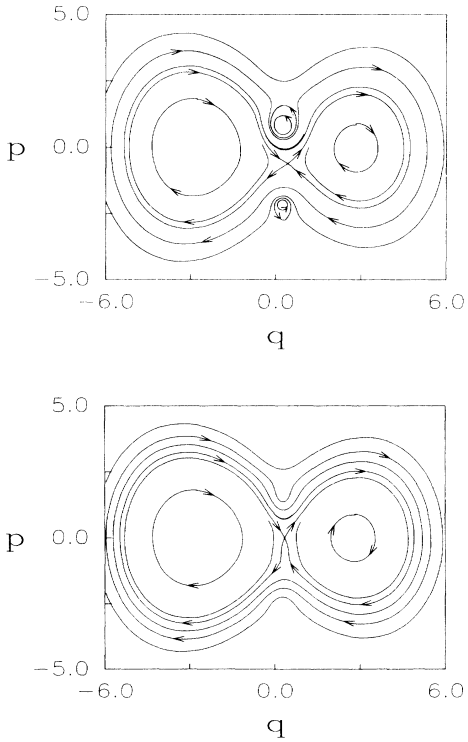

FIG. 3. Streamline trajectories for the superposition of the lowest pair of eigenstates of the double well at time $t=\tau_{\text{tun}}/5$. The upper panel shows the structure for the flux gauge $\delta\mathbf{J}=0$, while the lower panel shows the result for gauge (3.14).

neling time is sufficiently long to justify the separation of time scale assumption.

In Fig. 4, the quantum phase-space representation is depicted for six times during the half tunneling cycle $\{0,\tau_{\rm tun}/2\}$ obtained for the superposition of the lowest-energy pair of states. The left-hand panels in the figure show the development of the coherent-state density $\rho(p,q,t)$. Clearly, the density is localized in the left well at $t=0$ and smoothly evolves to the right well by $t=\tau_{\rm tun}/2$. The middle panels show the development of the instantaneous flux density $\mathbf{J}(p,q,t)$ at the same set of times. The right-hand panels contain representative sets of streamline trajectories propagated assuming that time is held fixed in the velocity field $\mathbf{v}(p,q,t)$.

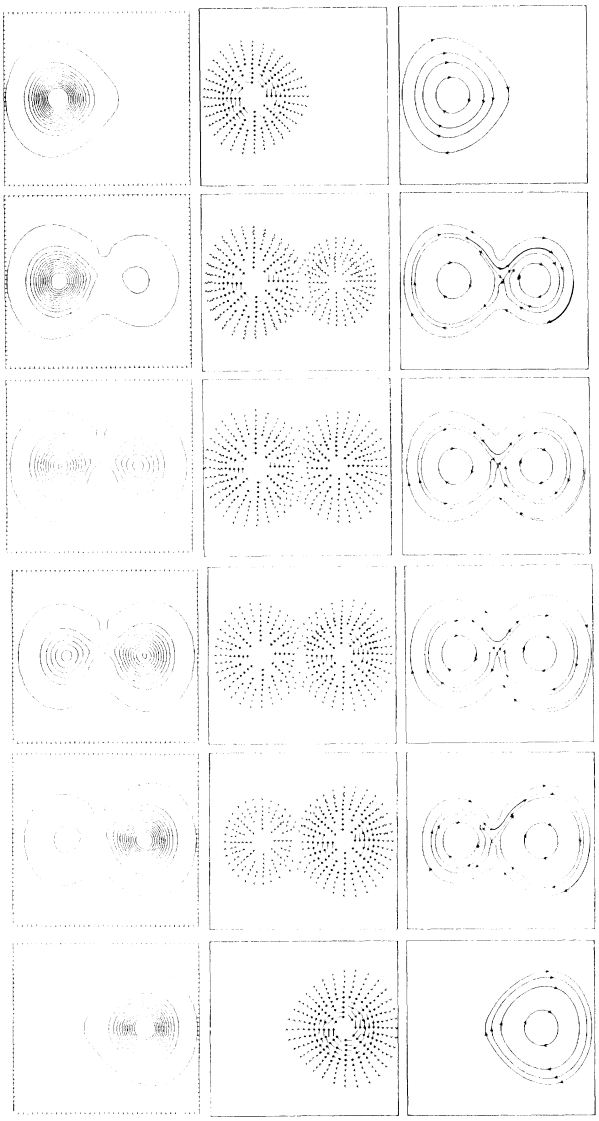

FIG. 4. Quantum phase-space structure for a superposition of the lowest pair of eigenstates of the double-well problem. The left-hand panels depict the density ρ at the set of six times $t=n\tau_{\rm tun}/10$, $n=0,1,2,3,4,5$. The middle panels show the (vector) flux density at these same times. In the right-hand panels, the streamline trajectories are plotted.

At $t=0$, the flux shows a circulation about a single (instantaneous) fixed point located near, but not precisely at, the minimum of the left-hand well. All the streamline orbits circulate about this one fixed point, even when passing over the region of the right-hand well, i.e., at positive q. At the later times, circulation sets in about a second fixed point located near the right potential minimum. A hyperbolic fixed point appears in the barrier region and denotes the boundary between the basins of circulation along the $p=0$ axis. The hyperbolic point and the right-hand elliptic point occur simultaneously via tangent bifurcation at a time near $t=0$. From the figure one also observes a region of circulation around the outside of all three fixed points. Thus one has three types of streamline trajectories, A, B, and C as in Fig. 1, which circulate about the left, right, and all three fixed points, respectively. Near the time $t=\tau_{\rm tun}/2$, when the entire wave packet has tunneled to the right well, the left elliptic point and the hyperbolic point disappear through an inverse tangent bifurcation and all circulation occurs about a single center near the right potential minimum.

For all times except during very brief intervals near the points $t=n\tau_{\rm tun}/2$ with $n=0,1,\ldots,$ there exist three fixed points in the instantaneous flow. With the choice of flux gauge given by Eq. (3.14), these instantaneous fixed points all lie on line $p=0$. An accurate numerical determination of their location (p_0,q_0), is made using a Newton search to solve $\mathbf{v}(p_0,q_0,\tau)=0$.

The behavior of the flow in the vicinity of one of these instantaneous fixed points may be discussed in terms of the linearized system,

$$\frac{d\Delta p}{dt}=\frac{\partial v_p(p_0,q_0,\tau)}{\partial q_0}\Delta q+\frac{\partial v_p(p_0,q_0,\tau)}{\partial p_0}\Delta p\ , \tag{4.5a}$$

$$\frac{d\Delta q}{dt}=\frac{\partial v_q(p_0,q_0,\tau)}{\partial q_0}\Delta q+\frac{\partial v_q(p_0,q_0,\tau)}{\partial p_0}\Delta p\ , \tag{4.5b}$$

with τ fixed and where

$$\Delta p=p-p_0,\quad \Delta q=q-q_0\ .$$

Equations (4.5) may be abbreviated using the z notation, where $\mathbf{z}\equiv(p,q)$, etc. In this notation, (4.5) becomes

$$\frac{d\Delta\mathbf{z}}{dt}=\mathbf{A}\cdot\Delta\mathbf{z}\ , \tag{4.6}$$

where $\mathbf{A}$ is the τ-dependent derivative matrix. The eigenvalue equation

$$\mathbf{A}\cdot\mathbf{z}_j=\lambda_j\mathbf{z}_j \tag{4.7}$$

defines the pure exponential motion along the instantaneous eigenvectors $\mathbf{z}_j$. The eigenvalue spectrum $\{\lambda_j\}$ may be used to classify the fixed point. Unlike with Hamiltonian dynamics, $\mathbf{A}$ does not have symplectic structure for the quantum problem except in the limit $\hbar\to 0$.

In the practical calculations, the 2×2 matrix $\mathbf{A}$ is obtained by numerical differentiation of the velocity field and the eigenvalue analysis is carried out. For the half

tunneling cycle shown in Fig. 6, the eigenvalues reveal that the left fixed point is an elliptic source and the right fixed point is an elliptic sink. That is, $\lambda_{\pm}$ are the complex eigenvalues from Eq. (4.7) with

$$\lambda_{\pm}=\lambda_R \pm i\lambda_I \ , \tag{4.8}$$

the fixed point is a source when $\lambda_R > 0$ and is a sink when $\lambda_R < 0$. Therefore the streamline orbits spiral outward from the source and spiral into the sink. The middle fixed point is a saddle point, i.e., a hyperbolic fixed point. It has two distinct eigenvalues λ_1 and λ_2 with $\lambda_1 > 0$ and $\lambda_2 < 0$. Unlike for Hamiltonian dynamics, one finds that here, generally,

$$\lambda_1+\lambda_2 \neq 0 \ ,$$

and thus areas are not preserved by the flow. During the second half cycle $\tau_{\text{tun}}/2 > t > \tau_{\text{tun}}$, during which probability flows back from right to left, the character of the elliptic points reverses and the right fixed point becomes the source and the left the sink.

The most important phase-space structure is that associated with the streamline manifolds from the hyperbolic fixed point. These manifolds are obtained, as in classical theory, by propagating orbits from near the fixed point along the eigenvectors of **A**. The two unstable branches are obtained by forward in time propagation while the two stable branches are obtained from backward in time propagation. Portions of the actual manifolds obtained in this way are pictured in the right panels of Fig. 4. To make the structure more visible, however, idealized versions of the manifolds at a time in the middle of each quarter tunneling cycle are shown in Fig. 5. Notice that relative positions of the stable and unstable manifolds interchange in going from first to the second quarter cycle. Exactly at $t = 0.25\tau_{\text{tun}}$ the manifolds actually join. During the first quarter cycle, trajectories spiral out of region A and into regions B and C. During the second quarter cycle, trajectories spiral into B from both A and C. During the second half tunneling cycle, the density flows back to A in a symmetrical fashion. Structures such as in Fig. 5 have been referred to elsewhere as "virtual separatrices."[73]

We can make use of the virtual separatrix in two ways. First, its manifolds divide quantum phase space into regions with distinct dynamical properties. In Fig. 6, closed regions A, B, and C, which are inhabited by the different type of streamline trajectories mentioned above, are defined in this way. Regions A and B, which lie inside the lobes of the virtual separatrix, correspond to probability density trapped in the left and right potential wells, respectively. Density in region C is the component of the state which is circulating above the barrier and is trapped in neither well. Note that the virtual separatrix does not close on itself, i.e., there are no simple homoclinic points. To define closed regions in phase space one must artificially close the regions. In the present problem this is accomplished by connecting the separatrix manifolds to the hyperbolic point with vertical straight lines $q = q_0$. This is physically reasonable here since the density is very low along this line.

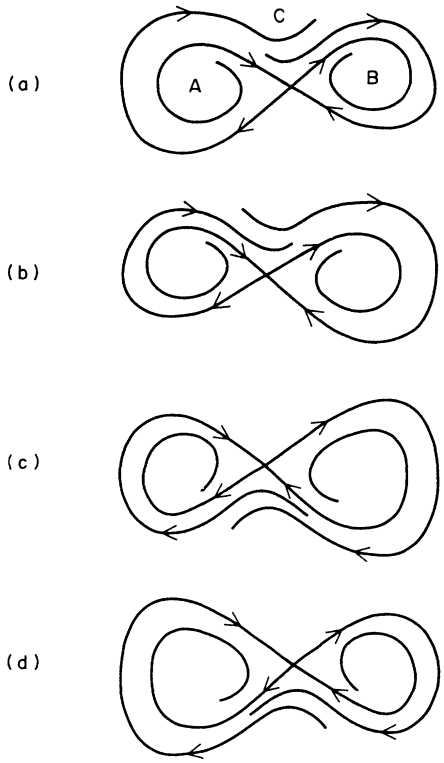

FIG. 5. An idealization of the manifolds from the hyperbolic point during each quarter cycle of the tunneling process. Regions A, B, and C are depicted.

A second use for the virtual separatrix is that it provides a means to quantitatively study transport in quantum phase space. Consider a scheme where one defines the distinct "species" A, B, and C using the virtual separatrix as above. A similar definition for dynamical species has been previously advanced in classical Hamiltonian mechanics.[74] Their concentrations at time t are given by

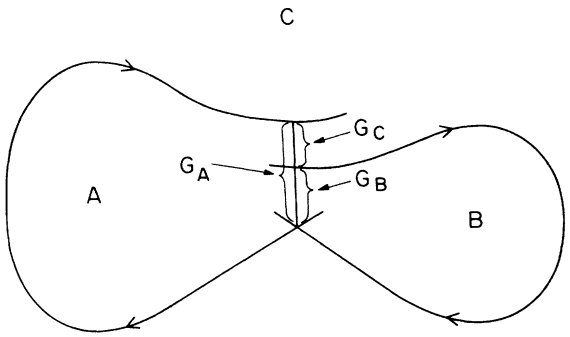

FIG. 6. Closed regions of quantum phase space for the first quarter cycle are defined using the virtual separatrix and a vertical line segment. The flux gates G_A, G_B, and G_C are depicted.

$$[A]=\int_A \rho\, dp\, dq \ , \tag{4.9a}$$

$$[B]=\int_B \rho\, dp\, dq \ , \tag{4.9b}$$

$$[C]=\int_C \rho\, dp\, dq \ , \tag{4.9c}$$

where the integrations are over the regions in the phase plane appropriate for each species. Thus we investigate the transport process by which these dynamically defined species interconvert between one another subject to the normalization condition

$$[A]+[B]+[C]=2\pi\hbar \ . \tag{4.10}$$

The time rate of change of a species, e.g., $[A]$, is given by

$$\frac{d[A]}{dt}=\int_A \frac{\partial\rho}{\partial t}dp\, dq+\int_{\mathcal{C}_A}\rho\mathbf{u}\cdot\mathbf{n}\, ds \ , \tag{4.11}$$

where $\mathcal{C}_A$ is the boundary curve to region A which is parametrized by s as $\{p_A(s),q_A(s)\}$, $\mathbf{u}$ is the time derivative of the curve $\mathcal{C}_A$, and $\mathbf{n}$ is the unit normal (pointing outward) to $\mathcal{C}_A$. The first term may be rewritten as

$$\begin{aligned}\int_A \frac{\partial\rho}{\partial t}dp\, dq &= -\int_A \nabla\cdot\mathbf{J}\, dp\, dq \\ &= -\oint_{\mathcal{C}_A}\mathbf{J}\cdot\mathbf{n}\, ds \ ,\end{aligned} \tag{4.12}$$

using the continuity equation and then the divergence theorem. Using $\mathbf{J}=\rho\mathbf{v}$, we have

$$\frac{d[A]}{dt}=\oint_{\mathcal{C}_A}\rho(\mathbf{u}-\mathbf{v})\cdot\mathbf{n}\, ds\equiv -F_A(t) \ , \tag{4.13}$$

which gives the rate of change of $[A]$, $-F_A(t)$ as a closed line integral around the boundary curve $\mathcal{C}_A$. In other words, $F_A(t)$ is the net flux out of A at time t. (Similar formulas hold for the concentrations $[B]$ and $[C]$.) The $\mathbf{v}$ term in the integral is the instantaneous flux across the static curve $\mathcal{C}_A$. The $\mathbf{u}$ term gives the rate of loss of density from region A due to the motion of the boundary curve $\mathcal{C}_A$ across the instantaneously static density distribution. When the tunneling time τ_{tun} is much longer than the typical vibrational period in the potential well τ_{vib}, then the virtual separatrix evolves slowly in time and one has

$$\|\mathbf{v}\| \gg \|\mathbf{u}\| \tag{4.14}$$

for all points on $\mathcal{C}_A$ except a set of small measure near the instantaneous fixed point. Recall that $\mathbf{v}$ must vanish at a pseudofixed point, while $\mathbf{u}$ may be nonzero. Thus for such deep tunneling cases, an accurate approximation to $F_A(t)$ is

$$F_A(t)\approx\oint_{\mathcal{C}_A}\rho\mathbf{v}\cdot\mathbf{n}\, ds \ , \tag{4.15}$$

which is the instantaneous flux across the static curve $\mathcal{C}_A$.

We now make a very important observation concerning the flux integral (4.15). Most of the curve $\mathcal{C}_A$ consists of an instantaneous streamline orbit along which $\mathbf{v}\perp\mathbf{n}$ and therefore $\mathbf{v}\cdot\mathbf{n}=0$. Thus the only nonzero contribution to the line integral (4.15) comes from the small segment connecting the hyperbolic point to the loose end of the separatrix manifold. This segment, denoted as G_A in Fig. 6, is what we term a "flux gate" since all the flux entering or exiting A must pass through this gate. Flux gates permit passage of flux in only one direction, either into or out of a closed region of quantum phase space. The flux gate construction is reminiscent of that of the turnstile[75] in Hamiltonian systems in that both provide a localized portal through which orbits transport between different regions of phase space.

The dominant component of the $\mathbf{u}$ part of the integral expression (4.13) for the exact flux $F_A(t)$ occurs at the flux gate. Therefore improved accuracy in the flux calculations may be achieved with very little added effort by including the uniform velocity of the flux gate $\mathbf{u}_A^0$, which is the same as the velocity of the fixed point, i.e., $(\dot{p}_0,\dot{q}_0)=(0,\dot{q}_0)=\mathbf{u}_A^0$. The flux gate approximation to the flux integral is therefore given by

$$F_A(t)\approx\int_{G_A}\rho(\mathbf{v}-\mathbf{u}_A^0)\cdot\mathbf{n}\, ds \ . \tag{4.16}$$

This is the expression used for the numerical calculations.

We note that there are different flux gates for the different regions G_A, G_B, and G_C and their topology changes as the virtual separatrix slowly evolves with time. During the first quarter cycle of the tunneling process $\tau_{\text{tun}}/4>t>0$, flux exits A and enters both B and C as shown in Fig. 7(a). Hence quantitatively

$$|F_A(t)|=|F_B(t)|+|F_C(t)| \ . \tag{4.17a}$$

During the second quarter cycle $\tau_{\text{tun}}/2>t>\tau_{\text{tun}}/4$, flux exits both A and C and enters B as in Fig. 7(b) and so

$$|F_B(t)|=|F_A(t)|+|F_C(t)| \ . \tag{4.17b}$$

At the halfway point, the source and sink interchange roles due to a rapid sequence of two tangent bifurcations and, so, during the third quarter cycle, Fig. 7(c), flux enters regions A and C and exits region B and we have

$$|F_B(t)|=|F_A(t)|+F_C(t)| \ . \tag{4.17c}$$

Finally, during the last quarter cycle, Fig. 7(d), flux enters A and leaves B and C and

$$|F_A(t)|=|F_B(t)|+|F_C(t)| \ . \tag{4.17d}$$

The flux density along the flux gate (and beyond) is shown in Fig. 8. Plotted as solid lines are $\mathbf{J}(p,q_0,t)\cdot\mathbf{n}=J_q(p,q_0,t)$ versus p at a set of 11 evenly spaced times in the quarter cycle $\tau_{\text{tun}}/4>t>0$. The distribution is seen to be bimodal at most times. The end points of the flux gates G_A and G_B at the various times are denoted with the dashed lines. It is perhaps an interesting coincidence that the flux gates seem to occur very near to the maximum of the flux density. One point is made very clear with this plot. Namely, only a fraction of the one-way flux across the line $q=q_0$ can be identified as flux out of region A, specifically that occurring between $p=0$ and the end point of the flux gate G_A. The remaining component of the flux at larger p values correspond to flux circulating in region C.

The concentrations as functions of time are obtained for the lowest pair of states by numerically solving the

differential equations

$$\frac{d[A]}{dt} = -F_A(t) ,$$
$$\frac{d[B]}{dt} = -F_B(t) , \qquad (4.18)$$
$$\frac{d[C]}{dt} = -F_C(t) ,$$

using the flux-gate approximation, Eq. (4.16), for the F's. In Fig. 9 the solutions to Eqs. (4.18) as functions of time are shown along with the exact concentrations obtained by direct phase-space integration of ρ as in Eqs. (4.9). The two are seen to agree to within about 1%, thus justifying the flux-gate picture of the tunneling transport for this system. If the u integrals along the separatrix manifolds are included in the flux expressions, $F_\gamma(t)$, Eq. (4.13), then the differential equations (4.18) should yield the exact concentrations as functions of time. We have numerically verified this to high precision as a consistency check on the method.

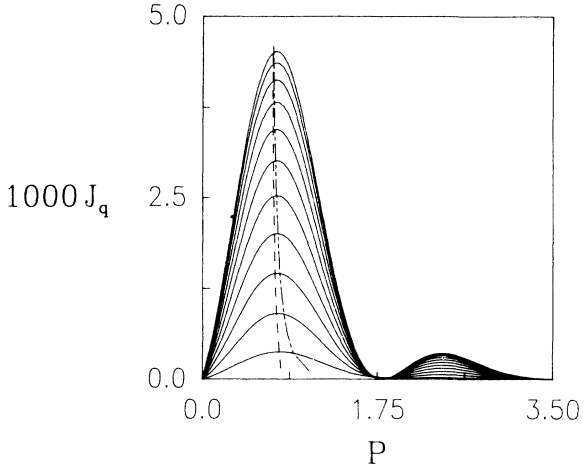

FIG. 8. Flux density J_q along the vertical line above the x point vs p. Plotted as solid lines are J_q at 11 equally spaced times during the first quarter cycle. The end point of the flux gate G_A at each time is shown with a dashed line, — — —, and the end point of G_B is shown with the line style—·—.

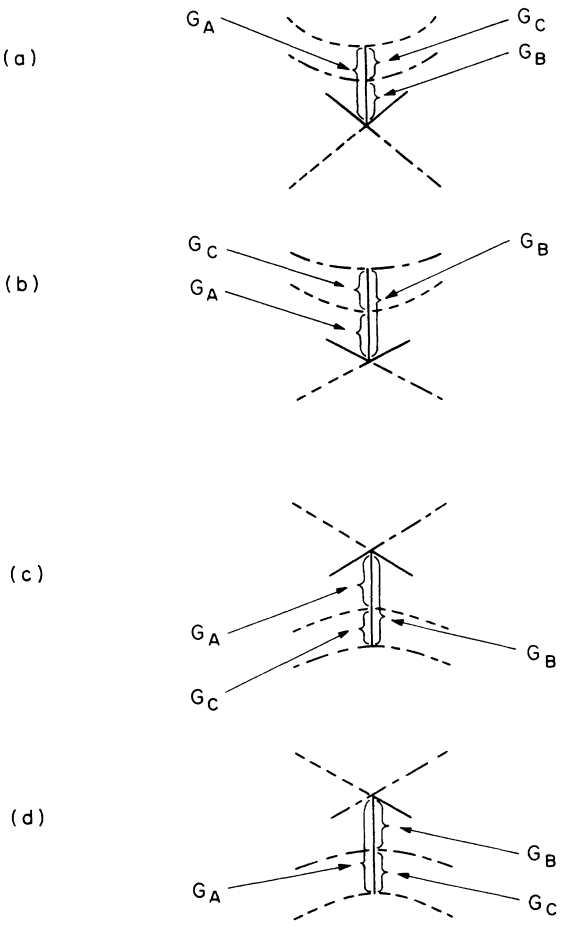

FIG. 7. Flux gates during each quarter tunneling cycle.

The physical picture that emerges for the tunneling process from the quantum phase-space approach is quite different than that obtained from the usual WKB or "instanton" semiclassical interpretation.[76] According to the latter, there are classically forbidden transitions between the quantized orbits lying in each well due to imaginary time trajectories which pass "through" the barrier after roughly $\tau_{\text{tun}}/\tau_{\text{vib}}$ oscillations on the classical KAM torus. In the phase-space hydrodynamic approach, the streamline trajectories spiral outward from the source well at a rate controlled by the tunneling time. At some point the trajectory passes through the flux gate and enters either the sink region or the external region C. For deep tun-

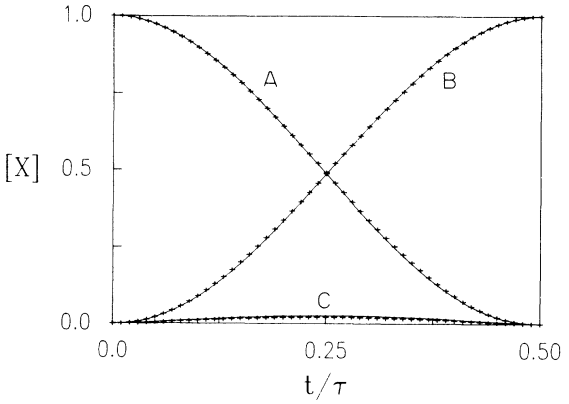

FIG. 9. Concentrations of species A, B, and C vs time. The crosses are the result of directly integrating ρ over the regions of phase space appropriate for A, B, and C. The solid lines are the result of solving the "kinetics equations" (4.18) using the flux-gate approximation for the rates $F_\gamma(t)$.

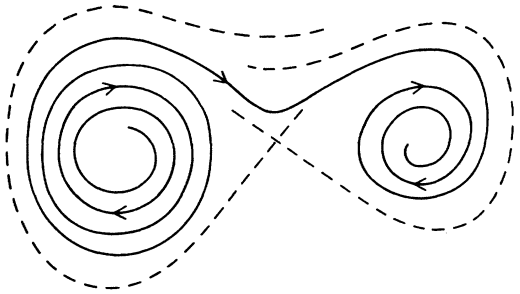

FIG. 10. A typical tunneling trajectory during the first half-cycle which spirals out of region A and into region B.

neling, the bulk of the flux goes directly from the source to the sink without passing into region C. Therefore the typical tunneling streamline trajectory spirals outward from the source and then inward toward the sink as shown in Fig. 10. Unlike in WKB theory, the tunneling takes place via real valued trajectories. The nonclassical tunneling phenomena come about due to non-Hamiltonian corrections to the equations of motion of order $O(\hbar)$ or higher.

It is interesting to compare the present analysis to a standard approach for the study of transport in classical phase space, namely, that afforded by transition-state theory (TST). This theory was introduced independently by Eyring and Wigner in the 1930s to provide a simple means to compute the rates of chemical reactions.[77] In TST, interconversion between distinct species is calculated by a one-way flux of a suitable statistical ensemble through a "critical configuration" (or transition state), which is a dividing surface that extends to infinity and topologically divides the different species. In the present problem, e.g., the conventional dividing surface would lie at the barrier $q=0$ with $p\in(0,\infty)$. Thus for such a TST analysis, only species A and B would exist.

One can imagine modifying TST to the study of transport in quantum phase space by calculating the flux through the transition state using the exact flux density. In the double-well problem, this TST rate for the loss of species A is

$$F_A^{\ddagger}(t)=\int_0^{\infty}\rho(p,q=0)\frac{p}{m}dp\ . \tag{4.19}$$

The rate obtained from (4.19) is plotted in Fig. 11(a) along with the exact rate and the flux-gate approximation. It is seen that the rate is greatly overestimated by this expression. The concentration $[A]$ obtained by a time integration of (4.19) is shown in Fig. 11(b) again with the exact and flux gate results. TST gives an overly rapid depletion of $[A]$ resulting eventually in spurious negative concentrations. There are two obvious problems with the TST expression. First, flux which is trapped in the wells and is circulating around in either region A ($t>\tau_{\rm tun}/4$) or region B ($\tau_{\rm tun}/2>t$) is misidentified as flux out of A. Second, the circulating flux in the outer region C is also misidentified as flux exiting A. The first source of error may be eliminated by relocating the TST dividing surface to the hyperbolic point $q=q_0$ with $p\in(0,\infty)$. This eliminates the "recrossing" of flux due to internal circulation in A and B. This modification is akin to the use of so called variational transition-state theory (VTST) where the dividing surface is moved to minimize recrossing. It is clear from Fig. 8, however, that most of the flux across even the relocated surface is misidentified flux from circulation in C. Indeed, as shown in Fig. 11 there remain serious errors in the rate and concentrations obtained from VTST.

Finally, we note that many aspects of the preceding treatment are not restricted only to states that are sums of pairs of symmetric and antisymmetric eigenstates such as Eq. (4.2). For example, in Fig. 12 we show the quantum phase-space representation for the state

$$|\Psi\rangle=\tfrac{1}{2}(|E_0\rangle e^{-iE_0t/\hbar}+|E_1\rangle e^{-iE_1t/\hbar}+|E_2\rangle e^{-iE_2t/\hbar}+|E_3\rangle e^{-iE_3t/\hbar}) \tag{4.20}$$

at a typical time. The quantum phase-space structure is

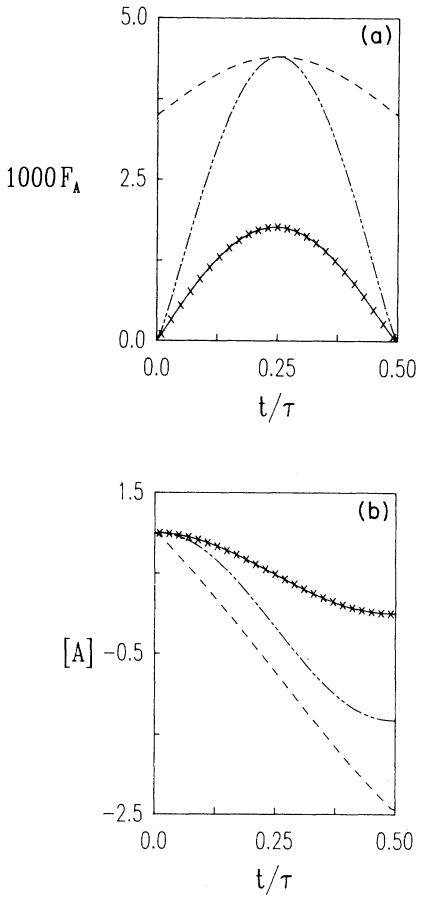

FIG. 11. (a) Rate and (b) concentration of species A as a function of time for comparison to TST. The $\times$'s are the exact results from direct integration of densities, while the solid line is the flux-gate approximation. The TST and VTST results are depicted with the line styles — — — and ----, respectively.

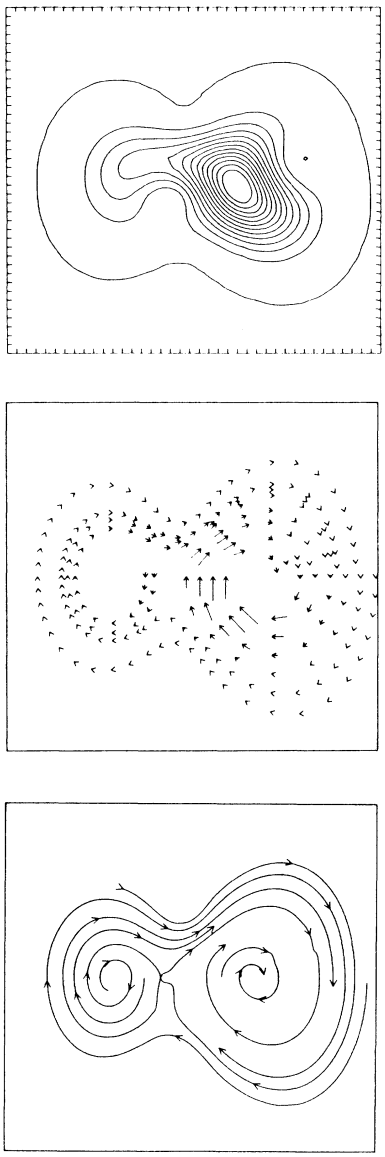

FIG. 12. Quantum phase-space structure for a superposition of the four lowest eigenstates for the double-well problem. The quantities depicted are the same as those in Fig. 4.

once again dominated by the manifolds from the saddle point. However, the flux-gate method for the computation of tunneling rates is less accurate ($\sim 10\%$ errors in rates) since the separation of time scales assumption does not hold as well for this state.

V. DISCUSSION AND CONCLUSIONS

The issue of classical quantum correspondence has been investigated by physicists with two broad purposes in mind. First, it is hoped that practical methods might be found to use classical mechanics to compute values for quantum-mechanical observables. Work in, e.g., WKB theory and EBK quantization has shown that significant computational advantage can be achieved in this way for certain problems. Second, and this what we have focused on here, it is of great interest to know to what extent the classical picture of dynamics carries over to the quantum world. We suggest that the hydrodynamic model provides an appropriate vehicle to study this question.

The key point about the hydrodynamic model is that it gives an exact, consistent, and classical-like picture for how the quantum phase-space density $\rho(\mathbf{p},\mathbf{q},t)$ evolves with time. Specifically, each "particle" of the indestructible density is transported along a Lagrangian fluid trajectory. The behavior of all the fluid trajectories can be organized by resolving the underlying structure of the quantum phase space using standard techniques available for first-order flows. In the limit $\hbar \to 0$, the structure becomes identical to the classical analog problem. For nonzero $\hbar$, quantum corrections appear of a generally non-Hamiltonian character. These correction terms depend on the state of the system just as do the "internal stresses" in a real fluid. By comparing the quantum to the classical phase-space structure the classical quantum correspondence may be accessed quantitatively for specific dynamical phenomena. Furthermore, our method permits a hydrodynamic interpretation of classical quantum differences such as the flux-gate picture of tunneling offered in Sec. IV.

There is, of course, inherent ambiguity in any quantum phase-space description due to the uncertainty principle. In the present treatment, the ambiguity is of two varieties. First, there is the unavoidable ambiguity implicit in all quantum phase-space theories due to the choice of representation for $\rho(\mathbf{p},\mathbf{q},t)$, e.g., Wigner, coherent state, etc. Second, and more specific to the present method, is the need to specify the flux gauge. This ambiguity is ultimately a factor ordering problem in the definition of the flux operators. We have advocated choosing the gauge to simplify the phase-space structure using the rationale that altering the flux densities in this way does not change the transport of ρ (since $\nabla \cdot \delta\mathbf{J} = 0$). Of course, while the net transport might not be affected, the choices of gauge may alter some of the details of the classical picture of the quantum dynamics. Therefore one goal for future work is to find a "unique" prescription for the flux gauge. One idea, discussed briefly in Sec. III C is to choose $\delta\mathbf{J}$ to make the quantum phase-space volume preserving under the flow when possible. Even this requirement, however, does not completely determine $\delta\mathbf{J}$. An obvious approach one might take is to construct $\hat{\mathbf{J}}$ from the classical expression using the particular correspondence rule appropriate for averaging with the specific choice of quantum phase-space representation. For example, the Weyl correspondence rules goes with the Wigner representation.[35] Unfortunately, however, it is not clear whether the continuity equation will always be satisfied with the resulting flux density. Despite the preceding discussion, though, we should emphasize that given a choice of representation and flux gauge, the resulting phase-space structure is unique and exact quantum-mechanical results may be reproduced in that formulation.

Finally, we consider generalizations and directions for future work. Although we have focused on one-dimensional problems here, there is in principle no problem in applying the hydrodynamic model in any number of degrees of freedom. Indeed, we have expended considerable effort to formulate the multidimensional flux expression, Eqs. (2.28)–(2.30). We intend, for one thing, to apply the model to multidimensional tunneling. We are also engaged in an application to the quantum standard map. Furthermore, we are interested in using the model to describe quantum reactive scattering.

ACKNOWLEDGMENTS

We are grateful to Michael J. Davis for useful comments and encouragement given during the course of this work. We are indebted to Robert Easton for his help in deriving one of the mathematical expressions. We have also profited from discussions with George Schatz, Donald Truhlar, and Alejandro Spina. This work was supported by Grant No. CHE-8609975 from the National Science Foundation. R.T.S. acknowledges receipt of financial support from the Sloan Foundation.

APPENDIX

In the configuration-space hydrodynamic model of pure states, the Madelung expression for the wave function

$$\Psi(\mathbf{x},t)=Ae^{iS/\hbar} \tag{A1}$$

proved a convenient form for the derivation of the fundamental relations (2.4) and (2.5). The "fluid" density is given by $\rho=A^2$, while S is a velocity-generating function where $\mathbf{v}=\nabla S/m$. When we extended the hydrodynamic model to mixed states and to quantum phase-space representations, we did not make use of this form. Instead, we directly derived the hydrodynamic relations for the density and flux density operators. In this appendix, we explore the possibility of using the Madelung form for these extensions of the hydrodynamic model.

We first consider the case of a mixed state in configuration space described by the density matrix $\rho(\mathbf{x},\mathbf{y},t)\equiv\langle\mathbf{x}|\hat{\rho}|\mathbf{y}\rangle$. In this off-diagonal representation, we believe the hydrodynamic model should be invoked in a $2N$-dimensional space where vectors have both x and y components. Thus the flux density is $\mathcal{J}=(\mathcal{J}_x,\mathcal{J}_y)$ and the velocity field is $\mathcal{V}=(\mathcal{V}_x,\mathcal{V}_y)$. We assume that the density may be written as

$$\rho(\mathbf{x},\mathbf{y},t)=B(\mathbf{x},\mathbf{y},t)e^{iR(\mathbf{x},\mathbf{y},t)/\hbar}\ , \tag{A2}$$

where B and R are real-valued functions. The density matrix is guaranteed to be Hermitian, $\rho(\mathbf{x},\mathbf{y},t)=\rho^*(\mathbf{y},\mathbf{x},t)$, by the conditions

$$B(\mathbf{x},\mathbf{y},t)=B(\mathbf{y},\mathbf{x},t) \tag{A3}$$

and

$$R(\mathbf{x},\mathbf{y},t)=-R(\mathbf{y},\mathbf{x},t)\ . \tag{A4}$$

Also, since $\rho(\mathbf{x},\mathbf{y},t)$ must be single valued, the contour integral of $R(\mathbf{x},\mathbf{y},t)$ around any closed path in $2N$-dimensional space must be an integral multiple of $2\pi\hbar$. The density matrix solves the Von Neumann equation,

$$i\hbar\frac{\partial\rho(\mathbf{x},\mathbf{y},t)}{\partial t}=-\frac{\hbar^2}{2m}[\nabla_x^2\rho(\mathbf{x},\mathbf{y},t)-\nabla_y^2\rho(\mathbf{x},\mathbf{y},t)] +[V(\mathbf{x})-V(\mathbf{y})]\rho(\mathbf{x},\mathbf{y},t)\ . \tag{A5}$$

Substituting the expression (A2) for the density matrix, the imaginary and real parts of the Von Neumann equation give

$$m\frac{\partial B}{\partial t}=-\nabla_x B\cdot\nabla_x R+\nabla_y B\cdot\nabla_y R-\tfrac{1}{2}B\nabla_x^2 R+\tfrac{1}{2}B\nabla_y^2 R\ , \tag{A6}$$

$$\frac{\partial R}{\partial t}=\frac{\hbar^2}{2mB}(\nabla_x^2 B-\nabla_y^2 B)-\frac{1}{2m}[(\nabla_x R)^2-(\nabla_y R)^2] -[V(\mathbf{x})-V(\mathbf{y})]\ . \tag{A7}$$

To make the hydrodynamic analogy, we need to relate the fluid density $\eta(\mathbf{x},\mathbf{y},t)$, and the flux density $\mathcal{J}(\mathbf{x},\mathbf{y},t)$ to the functions B and R. If we make the identifications

$$\eta=B^2\ , \tag{A8}$$

$$\mathcal{J}=\frac{\eta}{m}(\nabla_x R,-\nabla_y R)\ , \tag{A9}$$

then Eq. (A6) is the continuity equation

$$\frac{\partial\eta}{\partial t}=-\nabla\cdot\mathcal{J}\ , \tag{A10}$$

where $\nabla\equiv(\nabla_x,\nabla_y)$. If we act on both sides of Eq. (A7) with the differential operator $(\nabla_x,-\nabla_y)$, we obtain the $2N$-dimensional Euler-like equation,

$$\frac{\partial\mathcal{V}}{\partial t}+(\mathcal{V}\cdot\nabla)\mathcal{V}-(\mathcal{V}^\dagger\cdot\nabla)\mathcal{V}^\dagger =-\frac{\nabla V}{m}+\frac{\hbar^2}{2m^2}(\nabla-\nabla^\dagger)\frac{\nabla^2\sqrt{\eta}}{\sqrt{\eta}}\ , \tag{A11}$$

where

$$\mathcal{V}=\mathcal{J}/\eta,\quad \mathcal{V}^\dagger=(\mathcal{V}_y,\mathcal{V}_x),\quad \nabla^\dagger=(\nabla_y,\nabla_x)\ , \qquad \nabla V=[\nabla_x V(\mathbf{x}),\nabla_y V(\mathbf{y})]\ . \tag{A12}$$

Notice that (A11) differs from the pure-state Euler equation due to the presence of the terms with daggers.

It is interesting to compare the mixed-state hydrodynamic picture to the more familiar pure-state version. We show that the mixed-state formalism reduces to the usual formalism if we have a pure-state system. For pure-state quantum mechanics, $\rho(\mathbf{x},\mathbf{y},t)=\Psi^*(\mathbf{y},t)\Psi(\mathbf{x},t)$, or, in terms of the Madelung from (A1) we have

$$\rho(\mathbf{x},\mathbf{y},t)=A(\mathbf{x},t)A(\mathbf{y},t)\exp\{i[S(\mathbf{x},t)-S(\mathbf{y},t)]/\hbar\}\ . \tag{A13}$$

Thus we have the identifications

$$B(\mathbf{x},\mathbf{y},t)=A(\mathbf{x},t)A(\mathbf{y},t)\ , \tag{A14}$$

$$R(\mathbf{x},\mathbf{y},t)=S(\mathbf{x},t)-S(\mathbf{y},t)\ , \tag{A15}$$

which imply

$$\eta(\mathbf{x},\mathbf{y},t)=\rho(\mathbf{x},t)\cdot\rho(\mathbf{y},t)\ , \tag{A16}$$

$$\mathcal{J}(\mathbf{x},\mathbf{y},t)=[\mathbf{j}(\mathbf{x},t),\mathbf{j}(\mathbf{y},t)]\ , \tag{A17}$$

where $\rho(\mathbf{x},t)$ and $\mathbf{j}(\mathbf{x},t)$ are the pure-state hydrodynamic quantities given by Eqs. (2.6) and (2.7). Notice that, if the expressions (A16) and (A17) are used in the hydrodynamic equations (A10) and (A11), then upon separation of variables we immediately recover the pure-state formula (2.4) and (2.5'). Thus the mixed-state expressions reduce directly to the pure state as desired.

The Madelung form may also be adopted in the coherent-state representation. We consider only the pure-state case where we employ the form

$$\langle \mathbf{p},\mathbf{q}|\Psi\rangle = C(\mathbf{p},\mathbf{q},t)\cdot e^{iQ(\mathbf{p},\mathbf{q},t)/\hbar}\ , \tag{A18}$$

and C and Q are again real functions. The equations of evolution for C and Q may be determined from the coherent-state representation of the time-dependent Schrödinger equation

$$\langle \mathbf{p},\mathbf{q}|\hat{H}|\Psi\rangle = i\hbar\frac{\partial}{\partial t}\langle \mathbf{p},\mathbf{q}|\Psi\rangle\ . \tag{A19}$$

Using the expressions

$$\langle \mathbf{p},\mathbf{q}|\hat{\mathbf{P}}|\Psi\rangle = \left[\frac{\hbar}{i}\nabla_q+\frac{\mathbf{p}}{2}\right]\langle \mathbf{p},\mathbf{q}|\Psi\rangle \tag{A20}$$

and

$$\langle \mathbf{p},\mathbf{q}|\hat{\mathbf{x}}|\Psi\rangle = \left[-\frac{\hbar}{i}\nabla_p+\frac{\mathbf{q}}{2}\right]\langle \mathbf{p},\mathbf{q}|\Psi\rangle\ , \tag{A21}$$

it may be shown that (A19) becomes

$$\hat{H}\left[\frac{\hbar}{i}\nabla_q+\frac{\mathbf{p}}{2},-\frac{\hbar}{i}\nabla_p+\frac{\mathbf{q}}{2}\right]\langle \mathbf{p},\mathbf{q}|\Psi\rangle = i\hbar\frac{\partial}{\partial t}\langle \mathbf{p},\mathbf{q}|\Psi\rangle\ . \tag{A22}$$

Inserting the Madelung form (A18) into Eq. (A22) and assuming a Hamiltonian of the general form of Eq. (2.2), the imaginary and real parts of the resulting expression yield

$$m\frac{\partial C}{\partial t} = -\frac{1}{2}C\nabla_q^2 Q-\left[\nabla_q Q+\frac{\mathbf{p}}{2}\right]\cdot\nabla_q C + \frac{m}{\hbar}\mathrm{Im}\left[e^{-iQ/\hbar}V\left[-\frac{\hbar}{i}\nabla_p+\frac{\mathbf{q}}{2}\right]Ce^{iQ/\hbar}\right]\ , \tag{A23}$$

and

$$\frac{\partial Q}{\partial t} = \frac{\hbar^2}{2mC}\nabla_q^2 C-\frac{1}{2}\left[\nabla_q Q+\frac{\mathbf{p}}{2}\right]\cdot\nabla_q Q - \frac{1}{C}\mathrm{Re}\left[e^{-iQ/\hbar}V\left[-\frac{\hbar}{i}\nabla_p+\frac{\mathbf{q}}{2}\right]Ce^{iQ/\hbar}\right]-\frac{\mathbf{p}\cdot\mathbf{p}}{8m}\ . \tag{A24}$$

Thus we do not obtain simple hydrodynamic equations in this way unless V is a low-order polynomial in $\mathbf{x}$.

[1] *Stochastic Behavior in Classical and Quantum Hamiltonian Systems*, Vol. 93 of *Lecture Notes in Physics*, edited by G. Casati and J. Ford (Springer, Berlin, 1979).

[2] *Chaotic Behavior in Quantum Systems, Proceedings of the Conference on Quantum Chaos, Lake Como, Italy, 1983*, edited by G. Casati (Plenum, New York, 1985); *The Physics of Phase Space*, Vol. 278 of *Lecture Notes in Physics*, edited by Y. S. Kim and W. W. Zackary (Springer-Verlag, Berlin, 1986).

[3] J. E. Bayfield and P. M. Koch, Phys. Rev. Lett. **33**, 258 (1974); J. E. Bayfield and L. A. Pinnaduwage, *ibid.* **54**, 313 (1985); K. A. H. van Leeuen, G. V. Oppen, S. Renwick, J. B. Bowlin, P. M. Koch, R. V. Jensen, O. Rath, D. Richards, and J. G. Leopold, *ibid.* **55**, 2231 (1985).

[4] G. P. Berman and G. M. Zaslavskii, Phys. Lett. **61A**, 295 (1977); G. P. Berman and A. R. Kolovsky, Physica **8D**, 117 (1983).

[5] G. Casati, B. V. Chirikov, F. M. Izraelev, and J. Ford, in Ref. 1; F. M. Izraeleva and D. L. Shepelyanskii, Dokl. Akad. Nauk. SSSR **249**, 1103 (1979) [Sov. Phys.—Dokl. **24**, 996 (1979)].

[6] M. V. Berry, N. L. Balazs, M. Tabor, and A. Voros, Ann. Phys. (N.Y.) **122**, 26 (1979).

[7] K. G. Kay, J. Chem. Phys. **72**, 5955 (1980); **79**, 3026 (1983).

[8] J. S. Hutchinson and R. E. Wyatt, Chem. Phys. Lett. **72**, 378 (1980).

[9] H. J. Korsch and M. V. Berry, Physica **3D**, 627 (1981).

[10] Y. Weissman and J. Jortner, J. Chem. Phys. **77**, 1486 (1982).

[11] D. R. Grempel, S. Fishman, and R. E. Prange, Phys. Rev. Lett. **49**, 833 (1982); D. R. Grempel, R. E. Prange, and S. Fishman, Phys. Rev. A **29**, 1639 (1984).

[12] N. De Leon, M. J. Davis, and E. J. Heller, J. Chem. Phys. **80**, 794 (1984).

[13] E. J. Heller, Phys. Rev. Lett. **53**, 1515 (1984).

[14] R. V. Jensen, Phys. Rev. A **30**, 386 (1984).

[15] C. Jaffe and P. Brumer, J. Phys. Chem. **88**, 4829 (1984).

[16] T. Geisel, G. Radons, and J. Rubner, Phys. Rev. Lett. **57**, 2883 (1986); G. Radons, T. Geisel, and J. Rubner, Adv. Chem. Phys. **73**, 891 (1989).

[17] C. C. Martens and G. S. Ezra, J. Chem. Phys. **86**, 279 (1986).

[18] R. C. Brown and R. E. Wyatt, Phys. Rev. Lett. **57**, 1 (1986); R. C. Brown and R. E. Wyatt, J. Phys. Chem. **90**, 3590 (1986).

[19] R. G. Littlejohn, Phys. Rep. **138**, 193 (1986).

[20] S. J. Chang and K.-J. Shi, Phys. Rev. A **34**, 7 (1986).

[21] K. Takahashi, J. Phys. Soc. Jpn. **55**, 762 (1986); **55**, 1783 (1986).

[22] J. R. Cary, P. Rusu, and R. T. Skodje, Phys. Rev. Lett. **59**, 943 (1987).

[23] S. Fishman, D. R. Grempel, and R. E. Prange, Phys. Rev. A **36**, 289 (1987).

[24] L. L. Gibson, G. C. Schatz, M. A. Ratner, and M. J. Davis, J. Chem. Phys. **86**, 3263 (1987).

[25] S. K. Gray, J. Chem. Phys. **87**, 2051 (1987).

[26] G. Radons and R. E. Prange, Phys. Rev. Lett. **61**, 1691 (1988).

[27] W. A. Lin and L. E. Reichl, Phys. Rev. A **37**, 3972 (1988).

[28]R. Parson, J. Chem.. Phys. **89**, 262 (1988).
[29]M. J. Davis, J. Phys. Chem. **92**, 3124 (1988).
[30]R. S. MacKay and J. D. Meiss, Phys. Rev. A **37**, 4702 (1988).
[31]R. T. Skodje and J. R. Cary, Comp. Phys. Rep. **8**, 221 (1988).
[32]R. L. Waterland, J.-M. Yuan, C. C. Martens, R. E. Gillilan, and W. P. Reinhardt, Phys. Rev. Lett. **61**, 2733 (1988).
[33]E. Wigner, Phys. Rev. **40**, 749 (1932).
[34]K. Husimi, Proc. Phys. Math. Soc. Jpn. **22**, 264 (1940).
[35]J. E. Moyal, Proc. Cambridge Philos Soc. **45**, 99 (1949).
[36]T. Takabayasi, Prog. Theor. **11**, 341 (1954).
[37]A. O. Barut, Phys. Rev. **108**, 565 (1957).
[38]R. J. Glauber, Phys. Rev. **131**, 2766 (1963).
[39]J. R. Klauder, J. Math. Phys. **4**, 1055 (1963); **4**, 1058 (1963); **5**, 177 (1964).
[40]J. R. Klauder, E. C. G. Sudarshan, *Fundamentals of Quantum Optics* (Benjamin, New York, 1968).
[41]E. J. Heller, J. Chem. Phys. **62**, 1544 (1975); **65**, 1289 (1976); **66**, 5777 (1977); **67**, 3339 (1977).
[42]M. V. Berry, Philos. Trans. R. Soc. London, Ser. A **287**, 237 (1977).
[43]E. Prugovecki, Ann. Phys. (N.Y.) **110**, 102 (1978); *Stochastic Quantum Mechanics and Quantum Spacetime* (Reidel, Dordrecht, 1983).
[44]H. W. Lee and M. O. Scully, J. Chem. Phys. **73**, 2238 (1980); Found. Phys. **13**, 61 (1983); H. W. Lee and T. F. George, J. Chem. Phys. **84**, 6247 (1986); G. J. Milburn, Phys. Rev. A **33**, 674 (1986).
[45]V. I. Tatarskii, Usp. Fiz. Nauk. **139**, 587 (1983) [Sov. Phys.—Usp. **26**, 311 (1983)].
[46]E. B. Stechel and R. N. Schwartz, Chem. Phys. Lett. **83**, 350 (1981).
[47]N. L. Balazs and B. K. Jennings, Phys. Rep. **104**, 347 (1984).
[48]M. Hillery, R. F. O'Connell, M. O. Scully, and E. P. Wigner, Phys. Rep. **106**, 121 (1984).
[49]J. R. Klauder and B. Skagerstam, *Coherent States-Applications in Physics and Mathematical Physics* (World Scientific, Singapore, 1985).
[50]G. M. Zaslavsky, *Chaos in Dynamical Systems* (Harwood Academic, New York, 1985), Chaps. 9 and 10.
[51]P. D. Drummond and C. W. Gardiner, J. Phys. A: Math. Gen. **13**, 2353 (1980).
[52]S. W. McDonald, Phys. Rep. **158**, 339 (1988).
[53]B. Eckhardt, Phys. Rep. **163**, 207 (1988).
[54]M. C. Gutzwiller, J. Math. Phys. **11**, 1791 (1970); **12**, 343 (1971).
[55]E. Madelung, Z. Phys. **40**, 322 (1928).
[56]L. de Broglie, *An Introduction to the Study of Wave Mechanics* (Dutton, New York, 1930).
[57]P. A. M. Dirac, Proc. R. Soc. Lond, Ser. A **133**, 60 (1931).
[58]L. Landau, J. Phys. **5**, 71 (1941).
[59]F. London, Rev. Mod. Phys. **17**, 310 (1945).
[60]T. Takabayasi, Prog. Theor. Phys. **8**, 143 (1952); **9**, 187 (1953); **14**, 283 (1955).
[61]D. Bohm, Phys. Rev. **85**, 166 (1952); **85**, 180 (1952).
[62]J. Riess and H. Primas, Chem. Phys. Lett. **1**, 545 (1968); J. Riess, Ann. Phys. (N.Y.) **57**, 301 (1970); **67**, 347 (1971); Phys. Rev. D **2**, 647 (1970).
[63]H. E. Wilhelm, Phys. Rev. D **1**, 2278 (1970).
[64]J. H. Weiner and Y. Partom, Phys. Rev. **187**, 1134 (1969); J. H. Weiner and A. Askar, J. Chem. Phys. **54**, 3534 (1972); J. H. Weiner, *ibid.* **68**, 2492 (1978).
[65]E. A. McCullough and R. E. Wyatt, J. Chem. Phys. **54**, 3578 (1971).
[66]A. Kuppermann, J. T. Adams, and D. G. Truhlar, in *Abstracts of the Eighth International Conference of Physics of Electronic and Atomic Collisions, Belgrade, 1973,* edited by B. C. Cŏbić and M. V. Kurepa (Institute of Physics, Belgrade, 1973); J. M. Bowman, Ph.D. thesis, California Institute of Technology, 1975.
[67]J. O. Hirschfelder, A. C. Christoph, and W. E. Palke, J. Chem. Phys. **61**, 5435 (1974); J. O. Hirschfelder, C. J. Goebel, and L. W. Bruch, *ibid.* **61**, 5456 (1974); J. O. Hirschfelder and K. T. Tang, *ibid.* **64**, 760 (1976); **65**, 470 (1976).
[68]A. J. Lichtenberg and M. A. Lieberman, *Regular and Stochastic Motion* (Springer-Verlag, New York, 1983).
[69]J. Guckenheimer and P. Holmes, *Nonlinear Oscillations, Dynamical Systems, and Bifurcations of Vector Fields* (Springer-Verlag, New York, 1983).
[70]N. E. Kochin, I. A. Kibel, and N. V. Roze, *Theoretical Hydromechanics* (Interscience, New York, 1964); H. Lamb, *Hydrodynamics,* 6th ed. (Dover, New York, 1945).
[71]H. A. Kramers, *Quantum Mechanics,* translated by D. ter Haar, (North-Holland, Amsterdam, 1958); W. Pauli, *General Principles of Quantum Mechanics,* translated by P. Achuthan and K. Venkatesan (Springer-Verlag, Berlin, 1980).
[72]A. Messiah, *Quantum Mechanics* (Wiley, New York, 1961).
[73]R. H. Abraham and C. D. Shaw, *Dynamics—The Geometry of Behavior, Part Three: Global Behavior* (Aerial, Santa Cruz, 1985).
[74]S. K. Gray and S. A. Rice, J. Chem. Phys. **86**, 2020 (1987); R. T. Skodje, *ibid.* **90**, 6193 (1989).
[75]R. S. MacKay, and J. D. Meiss, and I. C. Percival, Physica **13D**, 375 (1984).
[76]R. Rajaraman, *Solitons and Instantons: An Introduction to Solitons and Instantons in Quantum Field Theory* (North-Holland, Amsterdam, 1982).
[77]For a recent review see, D. G. Truhlar, W. L. Hase, and J. T. Hynes, J. Phys. Chem. **87**, 2664 (1984). For a discussion of quantum transition-state theory see, W. H. Miller, J. Chem. Phys. **61**, 1823 (1974).